



Centrum voor Wiskunde en Informatica

REPORTRAPPORT

PNA

Probability, Networks and Algorithms



Probability, Networks and Algorithms

The Candy model revisited: Markov properties and inference

M.N.M. van Lieshout, R.S. Stoica

REPORT PNA-R0115 AUGUST 2001

CWI is the National Research Institute for Mathematics and Computer Science. It is sponsored by the Netherlands Organization for Scientific Research (NWO).

CWI is a founding member of ERCIM, the European Research Consortium for Informatics and Mathematics.

CWI's research has a theme-oriented structure and is grouped into four clusters. Listed below are the names of the clusters and in parentheses their acronyms.

Probability, Networks and Algorithms (PNA)

Software Engineering (SEN)

Modelling, Analysis and Simulation (MAS)

Information Systems (INS)

Copyright © 2001, Stichting Centrum voor Wiskunde en Informatica

P.O. Box 94079, 1090 GB Amsterdam (NL)

Kruislaan 413, 1098 SJ Amsterdam (NL)

Telephone +31 20 592 9333

Telefax +31 20 592 4199

ISSN 1386-3711

The Candy Model Revisited: Markov Properties and Inference

M.N.M. van Lieshout and R.S. Stoica

CWI

P.O. Box 94079, 1090 GB Amsterdam, The Netherlands

ABSTRACT

This paper studies the Candy model, a marked point process introduced by Stoica et al. (2000). We prove Ruelle and local stability, investigate its Markov properties, and discuss how the model may be sampled. Finally, we consider estimation of the model parameters and present some examples.

2000 Mathematics Subject Classification: 60G55, 62M40.

Keywords and Phrases: Candy model, Markov chain Monte Carlo simulation, Markov marked point process, maximum likelihood estimation, stability.

Note: Work carried out under project PNA4.3 ‘Stochastic Geometry’. This research was supported by NWO grant ‘Inference for random sets’ (613-03-045).

1. SET-UP AND NOTATION

In [36, 37], Stoica, Descombes and Zerubia introduced a marked point process model for line segments – dubbed *Candy* – as prior distribution for the image analysis problem of extracting linear networks such as roads or rivers from images (usually obtained by aerial photography or satellites). In this paper we investigate the analytical properties of the model, focusing on the Ruelle condition, local stability and the interaction structure. We also study statistical aspects, including simulation by Markov chain Monte Carlo and parameter estimation.

We shall represent a line segment as a point in some compact subset $K \subset \mathbb{R}^2$ of strictly positive volume $0 < \nu(K) < \infty$ with an attached mark taking values in the Cartesian product $[l_{\min}, l_{\max}] \times [0, \pi)$ for some $0 < l_{\min} < l_{\max} < \infty$. Each marked point (k, l, θ) can be interpreted as a line segment with midpoint k , length l , and orientation θ . If required, an extra mark for the width of the segment may be added. Note that in the original formulation [36, 37], the mark space for orientations is $[0, 2\pi]$.

A configuration of line segments is a finite set of marked points. Thus, for $n \in \mathbb{N}_0$, write S_n for the set of all (unordered) configurations $\mathbf{s} = \{s_1, \dots, s_n\}$ that consist of n , not necessarily distinct, marked points $s_i \in S = K \times [l_{\min}, l_{\max}] \times [0, \pi)$. Hence, the configuration space can be written as $\Omega = \cup_{n=0}^{\infty} S_n$, which may be equipped with the σ -algebra \mathcal{F} generated by the mappings $\{s_1, \dots, s_n\} \mapsto \sum_{i=1}^n 1\{s_i \in A\}$ that count the number of marked points in Borel sets $A \subseteq S = K \times [l_{\min}, l_{\max}] \times [0, \pi)$. If the marks are discarded, the configuration space of midpoints is $\Omega_K = \cup_{n=0}^{\infty} K_n$, where K_n is the set of all configurations $\mathbf{x} = \{k_1, \dots, k_n\}$ that consist of n , not necessarily distinct, points $k_i \in K$; the associated σ -algebra \mathcal{F}_K is generated by the mappings counting the number of points falling in Borel subsets of K .

A point process on K is a measurable mapping from some probability space into $(\Omega_K, \mathcal{F}_K)$; a marked point process with points in K and marks in $[l_{\min}, l_{\max}] \times [0, \pi)$ is a point process on the product space $K \times [l_{\min}, l_{\max}] \times [0, \pi)$ with the additional property that the marginal process of segment centers is a point process on K . For further details, see [4].

Perhaps the simplest marked point process model is the Poisson process defined by the probability measure

$$\mu(F) = \sum_{n=0}^{\infty} \frac{e^{-\nu(K)}}{n!} \{\pi(l_{\max} \Leftrightarrow l_{\min})\}^{-n} \int_S \cdots \int_S 1_F(\{(k_1, l_1, \theta_1), \dots, (k_n, l_n, \theta_n)\}) d\nu(k_1) \cdots d\nu(k_n) dl_1 \cdots dl_n d\theta_1 \cdots d\theta_n$$

on (Ω, \mathcal{F}) . In other words, under μ , midpoints are placed in K according to a Poisson process with intensity measure ν , to which points independent, uniformly distributed marks are assigned to determine the length and orientation. Exhibiting no interactions, the above Poisson marked point process is the ideal reference process. Indeed, one may define more complicated models by specifying a Radon–Nikodym derivative p with respect to μ . For the Candy model, at $\mathbf{s} = \{s_1, \dots, s_n\}$ with $s_i = (k_i, l_i, \theta_i) \in K \times [l_{\min}, l_{\max}] \times [0, \pi)$, $i = 1, \dots, n$,

$$p(\mathbf{s}) = \alpha \beta^{n(\mathbf{s})} \left\{ \prod_{i=1}^n \exp \left[\frac{l_i \Leftrightarrow l_{\max}}{l_{\max}} \right] \right\} \times \gamma_1^{n_f(\mathbf{s})} \gamma_2^{n_s(\mathbf{s})} \gamma_3^{n_r(\mathbf{s})} \gamma_4^{n_o(\mathbf{s})} \quad (1.1)$$

where $\gamma_1, \gamma_2, \gamma_3, \gamma_4 \in (0, 1)$ and $\beta > 0$ are the model parameters. Stoica et al. recommend $\gamma_1 < \gamma_2$. The sufficient statistics $n(\mathbf{s})$, $n_f(\mathbf{s})$, $n_s(\mathbf{s})$, $n_r(\mathbf{s})$, $n_o(\mathbf{s})$ represent respectively the total number of segments, the number of ‘free’ ones, the number of segments with a single one of its endpoints near another segment endpoint, the number of pairs of segments crossing at too sharp angles, and the number of pairs that are disoriented. A more precise definition will be given in section 2 below. Intuitively speaking, there are penalties attached to each free and singly connected segment, as well as to each sharp crossing and to every disagreement in orientation.

The plan of this paper is as follows. In section 2, a rigorous definition of the Candy model is given. We establish the Ruelle condition and local stability. Furthermore, we define several relations on the configuration space, and investigate the Markov behavior of the Candy model. In section 3, a Metropolis–Hastings algorithm based on births and deaths is suggested for sampling from the Candy model. We discuss the convergence of the algorithm, and prove geometric ergodicity. More sophisticated updates including non-uniform births and deaths, and changes in the marks are discussed subsequently. Section 4 builds on the results obtained in previous sections to perform maximum likelihood based inference. The paper is concluded by some examples.

2. THE CANDY MODEL: STABILITY AND MARKOV PROPERTIES

2.1 Model specification

The Candy model was developed in the context of a concrete image analysis problem [37], where, in order to decide whether two line segments were connected, discretization effects had to be taken into account. From a theoretical point of view, under the reference Poisson process almost surely no exact join between a pair of segments occurs. Such considerations motivate the following definition.

Definition 1. *Let $x = (k_x, l_x, \theta_x)$ and $y = (k_y, l_y, \theta_y)$ be two distinct marked points. Then,*

x and y are said to be connected if at least one of the following hold

$$\begin{aligned} \left\| \left(k_x + \frac{1}{2}l_x \cos \theta_x, k_x + \frac{1}{2}l_x \sin \theta_x \right) \Leftrightarrow \left(k_y + \frac{1}{2}l_y \cos \theta_y, k_y + \frac{1}{2}l_y \sin \theta_y \right) \right\| &\leq r_c \\ \left\| \left(k_x + \frac{1}{2}l_x \cos \theta_x, k_x + \frac{1}{2}l_x \sin \theta_x \right) \Leftrightarrow \left(k_y \Leftrightarrow \frac{1}{2}l_y \cos \theta_y, k_y \Leftrightarrow \frac{1}{2}l_y \sin \theta_y \right) \right\| &\leq r_c \\ \left\| \left(k_x \Leftrightarrow \frac{1}{2}l_x \cos \theta_x, k_x \Leftrightarrow \frac{1}{2}l_x \sin \theta_x \right) \Leftrightarrow \left(k_y + \frac{1}{2}l_y \cos \theta_y, k_y + \frac{1}{2}l_y \sin \theta_y \right) \right\| &\leq r_c \\ \left\| \left(k_x \Leftrightarrow \frac{1}{2}l_x \cos \theta_x, k_x \Leftrightarrow \frac{1}{2}l_x \sin \theta_x \right) \Leftrightarrow \left(k_y \Leftrightarrow \frac{1}{2}l_y \cos \theta_y, k_y \Leftrightarrow \frac{1}{2}l_y \sin \theta_y \right) \right\| &\leq r_c \end{aligned}$$

for some $r_c < l_{\min}$.

The relation of definition 1 is reflexive, that is any $x \in S$ is connected to itself. Similarly, an endpoint e of a segment x is said to be connected in the configuration \mathbf{s} if another segment in \mathbf{s} can be found with at least one endpoint closer than r_c to e . Following [36, 37], we distinguish between *singly connected* segments with exactly one connected endpoint and *doubly connected* ones for which both endpoints are connected. A segment that is not connected is said to be *free*.

Lemma 1. *The mappings n_f and n_s assigning to a configuration $\mathbf{s} \in \Omega$ the number of free, respectively singly connected segments are measurable with respect to \mathcal{F} .*

Proof: First, consider n_f . By its very nature, the mapping that counts the number of free segments in a configuration is a symmetric function of its argument. Thus, it is sufficient [30] to check that the function $f : S^n \rightarrow \mathbb{R}$ defined by

$$f(s_1, \dots, s_n) = \sum_{i=1}^n 1\{s_i \text{ is free}\}$$

is Borel measurable for each $n \in \mathbb{N}_0$. Now, for fixed $i \neq j \in \{1, \dots, n\}$, the function $f_{i,j}^1(s_1, \dots, s_n)$ defined by

$$1 \left\{ \left\| \left(k_i + \frac{1}{2}l_i \cos \theta_i, k_i + \frac{1}{2}l_i \sin \theta_i \right) \Leftrightarrow \left(k_j + \frac{1}{2}l_j \cos \theta_j, k_j + \frac{1}{2}l_j \sin \theta_j \right) \right\| > r_c \right\}$$

is Borel measurable as a mapping on S^n . Here, we use the notation $s_i = (k_i, l_i, \theta_i)$. Analogously, $f_{i,j}^2$, $f_{i,j}^3$ and $f_{i,j}^4$ defined similar to $f_{i,j}^1$ but using the second up to fourth condition of definition 1 instead of the first are Borel measurable. Consequently,

$$1\{s_i \text{ is free}\} = \prod_{j \neq i} \prod_{m=1}^4 f_{i,j}^m(s_1, \dots, s_n)$$

is Borel measurable, and so is the sum of these functions over i . A similar argument implies that n_s is measurable with respect to \mathcal{F} . \square

Next, define two neighborhood relations on S .

Definition 2. Let $\delta_{\min} > 0$. The relation \sim_r on S is defined by

$$x \sim_r y \Leftrightarrow \|k_x \Leftrightarrow k_y\| \leq \frac{\max\{l_x, l_y\}}{2} \text{ and } |\theta_x \Leftrightarrow \theta_y| \Leftrightarrow \pi/2| > \delta_{\min}$$

for any pair of distinct marked points $x = (k_x, l_x, \theta_x)$ and $y = (k_y, l_y, \theta_y)$.

The relation \sim_r is reflexive if $\delta_{\min} < \pi/2$.

Definition 3. The influence zone $Z(s)$ of a marked point $s = (k, l, \theta) \in S$ is given by

$$Z(s) = b \left(\left(k + \frac{1}{2}l \cos \theta, k + \frac{1}{2}l \sin \theta, \frac{1}{4}l \right) \cup b \left(\left(k \Leftrightarrow \frac{1}{2}l \cos \theta, k \Leftrightarrow \frac{1}{2}l \sin \theta, \frac{1}{4}l \right) \right),$$

the union of balls around the endpoints. The relation \sim_o on S is defined by $x \sim_o y \Leftrightarrow \|k_x \Leftrightarrow k_y\| > \frac{1}{2} \max\{l_x, l_y\}$ and **either** exactly one endpoint $(k_x \pm \frac{1}{2}l_x \cos \theta_x, k_x \pm \frac{1}{2}l_x \sin \theta_x)$ of x is a member of $Z(y)$ **or** exactly one endpoint $(k_y \pm \frac{1}{2}l_y \cos \theta_y, k_y \pm \frac{1}{2}l_y \sin \theta_y)$ of y is a member of $Z(x)$. Here $x = (k_x, l_x, \theta_x)$ and $y = (k_y, l_y, \theta_y)$ are distinct elements of S .

Note that \sim_o is not reflexive.

We are now ready to complete the specification of the sufficient statistics in (1.1). For a given configuration \mathbf{s} , write $n_r(\mathbf{s})$ for the number of \sim_r neighbor pairs in \mathbf{s} ; similarly $n_o(\mathbf{s})$ denotes the number of \sim_o neighbor pairs $\{x, y\}$ in \mathbf{s} with the extra property that

$$\min\{|\theta_x \Leftrightarrow \theta_y|, \pi \Leftrightarrow |\theta_x \Leftrightarrow \theta_y|\} > \tau_{\max} \tag{2.1}$$

for some threshold value $\tau_{\max} > 0$.

Lemma 2. The mappings n_r and n_o assigning to a configuration $\mathbf{s} \in \Omega$ the number of its \sim_r neighbor pairs, respectively the number of its \sim_o neighbor pairs satisfying (2.1) are measurable with respect to \mathcal{F} .

Proof: The counting of marked point pairs satisfying a certain condition is a symmetric operation. Regarding n_r , for each (x, y) , $1\{x \sim_r y\}$ is a Borel measurable function on S^2 , from which observation the result follows as in the proof of lemma 1. A similar, slightly more involved, argument applies to n_o . \square

We could have included (2.1) in the definition of \sim_o . The reason for not doing so is that in the ‘modified Candy model’ [36] both n_0 and the function n_a defined as the number of \sim_o neighbor pairs not satisfying the alignment property (2.1) are featured.

2.2 Stability

The existence of any point process specified in terms of an unnormalized, measurable density p with respect to a Poisson point process is ensured by Ruelle’s stability condition [7, 35]. This condition requires the energy $E(\mathbf{s}) = \Leftrightarrow \log(p(\mathbf{s})/p(\emptyset))$ to be bounded from below by a

linear term in the number of marked points in \mathbf{s} , i.e. $E(\mathbf{s}) \geq \Leftrightarrow Cn(\mathbf{s})$ for some $C > 0$, in which case the density (or the corresponding energy) is called *stable*. For the Candy model (1.1),

$$\begin{aligned} E(\mathbf{s}) &= \Leftrightarrow n(\mathbf{s}) \log \beta \Leftrightarrow \sum_{i=1}^{n(\mathbf{s})} \frac{l_i \Leftrightarrow l_{\max}}{l_{\max}} \\ &\Leftrightarrow n_f(\mathbf{s}) \log \gamma_1 \Leftrightarrow n_s(\mathbf{s}) \log \gamma_2 \Leftrightarrow n_r(\mathbf{s}) \log \gamma_3 \Leftrightarrow n_o(\mathbf{s}) \log \gamma_4 \\ &\geq \Leftrightarrow n(\mathbf{s}) \log \beta. \end{aligned}$$

If $\beta > 1$, take $C = \log \beta$; otherwise $E(\mathbf{s}) \geq 0 \geq \Leftrightarrow Cn(\mathbf{s})$ for any $C > 0$.

Theorem 1. *The unnormalized Candy density (1.1) is (Ω, \mathcal{F}) -measurable and integrable, hence specifies a well-defined marked point process.*

Proof: Measurability follows from lemmata 1–2, integrability is implied by the Ruelle condition, as

$$E_\mu \left[\frac{p(S)}{p(\emptyset)} \right] \leq \sum_{n=0}^{\infty} \frac{e^{-\nu(K)}}{n!} c^n \nu(K)^n = \exp[(c \Leftrightarrow 1)\nu(K)] < \infty.$$

□

A stronger stability condition is that of *local stability*, which requires the ratio $p(\mathbf{s} \cup \{\eta\})/p(\mathbf{s})$ to be uniformly bounded from above, both in $\mathbf{s} \in \Omega$ and $\eta \in S$, whenever $p(\mathbf{s}) > 0$.

Lemma 3. *The Candy model (1.1) is locally stable.*

Proof: Let $\mathbf{s} \in \Omega$, and $\eta = (k, l, \theta) \in S$. Since $p > 0$, the ratio $p(\mathbf{s} \cup \{\eta\})/p(\mathbf{s})$ is well-defined. Clearly, the addition of η results in an extra term $\beta \exp\{(l \Leftrightarrow l_{\max})/l_{\max}\} \leq \beta$ regardless of the position of η with respect to \mathbf{s} . The effect on the other four terms does depend on the type of connections introduced by η , which we investigate separately below.

First consider $n_f(\mathbf{s} \cup \{\eta\}) \Leftrightarrow n_f(\mathbf{s})$. If η is not connected to any segment in \mathbf{s} , the difference in free segments is 1. If η is singly connected, say through its endpoint e , by the addition of η to \mathbf{s} the number of free segments decreases by the number of segments connected to e that were free in \mathbf{s} ; since at most 6 segment endpoints separated by at least a distance r_c can be placed in a ball of radius r_c centered at e , in this case $n_f(\mathbf{s} \cup \{\eta\}) \Leftrightarrow n_f(\mathbf{s}) \geq \Leftrightarrow 6$. Analogously, for doubly connected segments η , $n_f(\mathbf{s} \cup \{\eta\}) \Leftrightarrow n_f(\mathbf{s}) \geq \Leftrightarrow 12$.

Next, turn to $n_s(\mathbf{s} \cup \{\eta\}) \Leftrightarrow n_s(\mathbf{s})$. If η is free, the number of singly connected segments does not change. If η is singly connected through its endpoint e , since the status of segments not connected to η is not affected, we have to examine segments connected to e . Now, segments that were free with respect to \mathbf{s} get singly connected in $\mathbf{s} \cup \{\eta\}$; if both endpoints of a segment were connected in \mathbf{s} , so are they in $\mathbf{s} \cup \{\eta\}$. Segments for which the endpoint connected to e was also connected in \mathbf{s} and the other endpoint was free in \mathbf{s} remain singly connected in the new configuration $\mathbf{s} \cup \{\eta\}$. On the other hand, a segment that was singly connected in \mathbf{s} but whose \mathbf{s} -free endpoint is connected to e becomes doubly connected after the addition of η . Hence $n_s(\mathbf{s} \cup \{\eta\}) \Leftrightarrow n_s(\mathbf{s})$ increases by 1 plus the number of free members of \mathbf{s} , and decreases by the number of segments that were singly connected in \mathbf{s} with the free endpoint connected to e . Since there could be at most 6 segments of the latter type, $n_s(\mathbf{s} \cup \{\eta\}) \Leftrightarrow n_s(\mathbf{s}) \geq \Leftrightarrow 5$.

In case η is doubly connected, again we may restrict ourselves to considering the status of segments connected to η . As before, $n_s(\mathbf{s} \cup \{\eta\}) \Leftrightarrow n_s(\mathbf{s})$ decreases by at most (since both endpoints of a segment $s \in \mathbf{s}$ could be connected to η) the number of segments that were singly connected in \mathbf{s} with the free endpoint connected to η , a number that is bounded by 12.

Finally, note that $n_r(\mathbf{s} \cup \{\eta\}) \geq n_r(\mathbf{s})$ and $n_o(\mathbf{s} \cup \{\eta\}) \geq n_o(\mathbf{s})$. If we collect all terms examined above, we obtain

$$\frac{p(\mathbf{s} \cup \{\eta\})}{p(\mathbf{s})} \leq \beta(\gamma_1 \gamma_2)^{-12}$$

and the proof is complete. \square

2.3 Markov properties

A marked point process is said to be Ripley–Kelly Markov [31] with respect to some symmetric relation \sim on S if its density is hereditary (that is $p(\mathbf{s}) > 0$ implies $p(\mathbf{s}') > 0$ for all $\mathbf{s}' \subseteq \mathbf{s}$), and if for all \mathbf{s} such that $p(\mathbf{s}) > 0$, and all $\eta \notin \mathbf{s}$, the ratio $p(\mathbf{s} \cup \{\eta\})/p(\mathbf{s})$ depends only on η and those $s \in \mathbf{s}$ satisfying $s \sim \eta$. In physical terms, the energy required to add η to \mathbf{s} depends only on η and its \sim -neighbors in \mathbf{s} . See the recent monograph [20] for further details.

Proposition 1. *For $\gamma \in (0, 1)$, the partial Candy model with probability density*

$$p(\mathbf{s}) \propto \gamma^{n_r(\mathbf{s})}, \quad \mathbf{s} \in \Omega,$$

with respect to μ is Markov with respect to the relation \sim_r .

Proof: The density is strictly positive, hence hereditary. Furthermore, for $\eta \notin \mathbf{s} \in \Omega$,

$$\frac{p(\mathbf{s} \cup \{\eta\})}{p(\mathbf{s})} = \gamma^{n_r(\mathbf{s} \cup \{\eta\}) - n_r(\mathbf{s})} = \gamma^{n(\{s \in \mathbf{s} : s \sim_r \eta\})}$$

depends only on the number of \sim_r -neighbors of η in \mathbf{s} . \square

Proposition 2. *For $\gamma \in (0, 1)$, the partial Candy model with probability density*

$$p(\mathbf{s}) \propto \gamma^{n_o(\mathbf{s})}, \quad \mathbf{s} \in \Omega,$$

with respect to μ is Markov with respect to the relation \sim_o .

As an aside, it should be noted that a similar result could be derived for the modified Candy model.

Proof: The density is strictly positive, hence hereditary. Furthermore, for $\eta = (k_\eta, l_\eta, \theta_\eta) \notin \mathbf{s} \in \Omega$,

$$\frac{p(\mathbf{s} \cup \{\eta\})}{p(\mathbf{s})} = \gamma^{n_o(\mathbf{s} \cup \{\eta\}) - n_o(\mathbf{s})} = \gamma^{n(\{s = (k_s, l_s, \theta_s) \in \mathbf{s} : s \sim_o \eta; \min\{|\theta_\eta - \theta_s|, \pi - |\theta_\eta - \theta_s|\} > \tau_{\max}\})}$$

depends only on η and its \sim_o -neighbors in \mathbf{s} . \square

Both the model of proposition 1 and that of proposition 2 exhibit pairwise interactions only, that is factorize according to

$$p(\mathbf{s}) = p(\emptyset) \prod_{s_i \sim s_j} \phi(s_i, s_j)$$

where \sim is either \sim_r or \sim_o . The function $\phi(s_i, s_j)$ takes the constant value γ for the partial Candy model of proposition 1; for the model in proposition 2,

$$\phi(s_i, s_j) = \gamma^{1\{\min\{|\theta_{s_i} - \theta_{s_j}|, \pi - |\theta_{s_i} - \theta_{s_j}|\} > \tau_{\max}\}}.$$

The statistics n_f and n_s call for a configuration dependent Markov property [1], since in order to decide whether a given segment is free, singly, or doubly connected, one needs to examine the segments connected to it. The two-step iterated neighbors relation, also studied in [18, 13] is defined as follows. Based on the relation \sim_c on S defined by $x \sim_c y$ if and only if x and y are connected (definition 1), set

$$x \sim_s^2 y \Leftrightarrow x \sim_c y \text{ or } \exists z \in \mathbf{s} : x \sim_c z \sim_c y$$

for $x, y \in S$ and $\mathbf{s} \in \Omega$. A point process with density p is nearest-neighbor Markov [1] with respect to \sim^2 in the sense of Baddeley and Møller if p is hereditary, and if for any configuration \mathbf{s} such that $p(\mathbf{s}) > 0$, and all $\eta \notin \mathbf{s}$, the ratio $p(\mathbf{s} \cup \{\eta\})/p(\mathbf{s})$ depends only on η , its two-step iterated neighbors in $\mathbf{s} \cup \{\eta\}$, and the relations \sim_s^2 and $\sim_{\mathbf{s} \cup \{\eta\}}^2$ restricted to this neighborhood. Although the first consistency condition of Baddeley and Møller [1] (requiring that if \mathbf{s} is not a clique in some $\mathbf{s}' \supseteq \mathbf{s}$ but is in $\mathbf{s}' \cup \{u\}$, then \mathbf{s} contains only $\sim_{\mathbf{s}' \cup \{u\}}^2$ neighbors of u) does not hold [20], so that two-step pairwise interaction models are ruled out, the following theorem concerns an example of a point process that is nearest-neighbor Markov with respect to \sim^2 .

Theorem 2. *For $\gamma_1, \gamma_2 \in (0, 1)$, the partial Candy model with probability density*

$$p(\mathbf{s}) \propto \gamma_1^{n_f(\mathbf{s})} \gamma_2^{n_s(\mathbf{s})}, \quad \mathbf{s} \in \Omega,$$

with respect to μ is two-step iterated neighbors Markov with respect to the relation \sim_c on S .

Proof: By the proof of lemma 3,

$$\gamma_1^{n_f(\mathbf{s} \cup \{\eta\}) - n_f(\mathbf{s})}$$

depends only on the status of η and that of the segments connected to it. To decide the status of η , knowledge of its \sim_c -neighbors suffices; to assess the connection type of these neighbors, their neighbors have to be taken into account. The same is true for

$$\gamma_2^{n_s(\mathbf{s} \cup \{\eta\}) - n_s(\mathbf{s})}.$$

Consequently, p is a two-step iterated neighbors Markov point process with respect to the connection relation \sim_c . \square

As a consequence of propositions 1–2 and theorem 2, the Candy model is Markov at fixed range $2(l_{\max} + r_c)$ regardless of the marks, i.e. with respect to the relation \sim defined by

$$x \sim y \Leftrightarrow |k_x \Leftrightarrow k_y| \leq 2(l_{\max} + r_c).$$

3. METROPOLIS–HASTINGS ALGORITHMS

3.1 Review

The Candy model (1.1) is too complicated to sample from directly. Rather, we apply Markov chain Monte Carlo techniques [9, 12, 24] to construct a Markov chain that has the Candy model as its equilibrium distribution π , i.e.

$$\pi(F) = \int_F p(\mathbf{s})\mu(ds) \quad (3.1)$$

for all $F \in \mathcal{F}$; as before, μ denotes the distribution of the reference Poisson process. An example of such a Markov chain is the Metropolis–Hastings sampler, originally introduced in statistical physics [2, 21]. It is a flexible proposal-acceptance technique [17, 27] that is well adapted to point processes [10, 14, 25]. In that context, transitions much at least include births and deaths. The generic choice is as follows. Suppose a birth is proposed with probability p_b , and a death with the complimentary probability $p_d = 1 \Leftrightarrow p_b$. In case of a birth, a new segment is sampled uniformly, so that the birth proposal density can be written as

$$b(\mathbf{s}, \eta) = \frac{1}{\nu(K)}, \quad s \in \Omega, \eta \in S, \quad (3.2)$$

with respect to the product $d\sigma(\eta) = (\nu(dk) dl d\theta)/(\pi(l_{\max} - l_{\min}))$ of Lebesgue measure on K and uniform distributions on $[l_{\min}, l_{\max}]$ and $[0, \pi)$. It should be noted that (3.2) does not depend on the current configuration \mathbf{s} . The probability mass function of death proposals for points $\eta \in \mathbf{s}$ is given by

$$d(\mathbf{s}, \eta) = \frac{1}{n(\mathbf{s})} \quad (3.3)$$

for $\mathbf{s} \neq \emptyset$, and each point η has the same probability of being removed. In case $\mathbf{s} = \emptyset$, the new state is empty too.

A transition from \mathbf{s} to \mathbf{s}' is subsequently accepted with probability $\alpha(\mathbf{s}, \mathbf{s}')$. The detailed balance equations require that, under the target equilibrium density p , the addition of $\eta \in S$ to $\mathbf{s} \in \Omega$ is matched by a death of η from $\mathbf{s} \cup \{\eta\}$, that is

$$p_b b(\mathbf{s}, \eta) \alpha(\mathbf{s}, \mathbf{s} \cup \{\eta\}) p(\mathbf{s}) = p_d d(\mathbf{s} \cup \{\eta\}, \eta) \alpha(\mathbf{s} \cup \{\eta\}, \mathbf{s}) p(\mathbf{s} \cup \{\eta\}). \quad (3.4)$$

A solution is

$$\alpha(\mathbf{s}, \mathbf{s} \cup \{\eta\}) = \min \left\{ 1, \frac{p_d d(\mathbf{s} \cup \{\eta\}, \eta) p(\mathbf{s} \cup \{\eta\})}{p_b b(\mathbf{s}, \eta) p(\mathbf{s})} \right\} \quad (3.5)$$

with $\alpha(\mathbf{s} \cup \{\eta\}, \mathbf{s})$ given by substitution of (3.5) into (3.4). By the results in [10, section 4], the algorithm converges in total variation to π for π -almost all initial configurations provided $p_b \in (0, 1)$. The theorem applies equally to any pair of strictly positive proposal distributions, not necessarily equal to (3.2)–(3.3).

3.2 Tailor-made updates

Connection-dependent transitions

Stoica et al. [36, 37] used the following updates:

- birth and death of a free segment;
- birth and death of a singly connected segment with a single \sim_c -neighbor;
- birth and death of a singly connected segment with at least two \sim_c -neighbors;
- birth and death of a doubly connected segment.

Clearly, such moves are tailored to obtain connected configurations, but the subsets of S to which new segments of a given type must belong are quite complicated. Thus, [36, 37] felt forced to use approximations (both of the proposal density and the acceptance ratio) that jeopardize the convergence of the Markov chain to the correct target distribution.

A more tractable alternative is to design a probability density that tends to propose segments near to and aligned with the current network. The idea is that preference should be given to positions that ‘fit’ the current configuration. More specifically, a new segment might be positioned in such a way that it extends the current configuration.

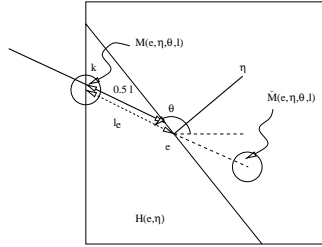


Figure 1: How to extend the network.

Let us consider an endpoint e of a segment η , cf. figure 1. To sample a segment connected to e , we begin by choosing an orientation θ , say according to a probability density f with respect to the uniform distribution on $[0, \pi)$. Let $H(e, \eta)$ be the half-open half plane at e orthogonal to η that does not contain η . Now, since the center of the new segment must be an element of the set $K \cap H(e, \eta)$, the segment length cannot exceed twice the distance $l_{e, \eta}(\theta)$ of e to K^c along the line through e with orientation θ restricted to the half plane $H(e, \eta)$. Consequently, conditional on θ , we assume the length law to possess a density $g(\cdot | e, \eta, \theta)$ with respect to the uniform distribution on $[l_{\min}, l_{\max}]$ that is concentrated on $[l_{\min}, \min\{2l_{e, \eta}(\theta), l_{\max}\}]$. The update is completed by generating a midpoint k , uniformly or otherwise, on $M(e, \eta, \theta, l) = b(e \pm l(\cos \theta, \sin \theta)/2, r_c) \cap K$, the sign chosen so as to belong to $H(e, \eta)$. We will denote the probability density with respect to ν by $h(k | e, \eta, \theta, l)$. Clearly, the birth is possible only if the interval $[l_{\min}, \min\{2l_{e, \eta}(\theta), l_{\max}\}]$ and the set $M(e, \eta, \theta, l)$ both have strictly positive Lebesgue measure. In that case, the proposal density at endpoint e of segment η is given by

$$\tilde{b}(e, \eta, (k, l, \theta)) = h(k | e, \eta, \theta, l) g(l | e, \eta, \theta) f(\theta) \quad (3.6)$$

where $\theta \in [0, \pi)$, $l \in [l_{\min}, \min\{2l_{e,\eta}(\theta), l_{\max}\}]$, and $k \in M(e, \eta, \theta, l)$; otherwise, $\tilde{b}(e, \eta, (k, l, \theta)) = 0$. In summary, provided $A(\mathbf{s}) \neq \emptyset$ for $\mathbf{s} \in \Omega$, the proposal density for prolonging the segment configuration \mathbf{s} is given by the average

$$b_p(\mathbf{s}, (k, l, \theta)) = \frac{1}{n(A(\mathbf{s}))} \sum_{(e,\eta) \in A(\mathbf{s})} \tilde{b}(e, \eta, (k, l, \theta)) \quad (3.7)$$

of (3.6) over $A(\mathbf{s})$, the set of endpoint-segment pairs (e, η) , $\eta \in \mathbf{s}$, allowing addition of a new segment to e . If $n(A(\mathbf{s})) = 0$, a uniformly distributed birth is proposed.

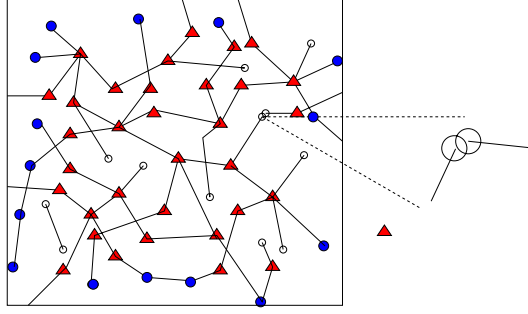


Figure 2: Extremities marked by triangles are connected and further than $\frac{1}{2}l_{\max} + r_c$ to the boundary, those labeled by a black disk are closer than $\frac{1}{2}l_{\max} + r_c$ to the boundary of K .

Examples of (3.6) include uniform updates

$$\begin{aligned} f(\theta) &= 1; \\ g(l|e, \eta, \theta) &= \frac{(l_{\max} - l_{\min}) \mathbb{1}\{l \in [l_{\min}, \min\{2l_{e,\eta}(\theta), l_{\max}\}]\}}{\min\{2l_{e,\eta}(\theta), l_{\max}\} - l_{\min}}; \\ h(k|e, \eta, \theta) &= \frac{\mathbb{1}\{k \in M(e, \eta, \theta, l)\}}{\nu(M(e, \eta, \theta, l) \cap K)}, \end{aligned} \quad (3.8)$$

again assuming non-zero denominators. Alternatively, the orientation could be centered around that of η , for example by means of a Beta distribution, to favor a better alignment.

In the simulations of section 5 we connect only to segment endpoints $e \in \eta$ further than $\frac{1}{2}l_{\max} + r_c$ away from K^c ; the current connections to e may be taken into account as well, as illustrated in figure 2. With this convention, for any θ , $g(\cdot|e, \eta, \theta)$ may be positive on the maximal interval $[l_{\min}, l_{\max}]$ and the putative midpoint is sampled on a full ball of area πr_c^2 .

Back bends, although penalized by the model for most values of γ_A and τ_{\max} (see (2.1)), may be formalized by sampling a new center in $H(e, \eta)^c$ as indicated in figure 1. Note that the two directed distances to the boundary of K along a line through e with orientation θ may well be different, leading to conditional length distributions that are concentrated on different supports. In practice, we restrict ourselves to extremities that are far away from the boundary, hence both distributions are concentrated on the full support $[l_{\min}, l_{\max}]$. Thus, a mixture proposal distribution for prolongations and back bends could take the following form. Choose an orientation θ according to a probability density f with respect to the uniform distribution on $[0, \pi)$. Conditionally given θ , the length is sampled according to a density $g(\cdot|e, \eta, \theta)$ with respect to the uniform distribution on $[l_{\min}, l_{\max}]$. Finally, with probability

p_M a midpoint is sampled on $M(e, \eta, \theta, l)$, say uniformly; with the complementary probability $1 \Leftrightarrow p_M$, a center is generated on $\tilde{M}(e, \eta, \theta, l)$.

Modifying the segment characteristics

To improve the mixing of the Markov chain, apart from adapting the birth proposal density to the target density, a common strategy is to include transition types other than births and deaths. Thus, in [36, 37], the following updates are considered:

- changing the orientation of a singly connected segment;
- changing the length of a singly connected segment;
- changing the position of a singly connected segment with a single \sim_c -neighbor;
- changing the position of a singly connected segment with at least two \sim_c -neighbors.

The partition in connection types has the same drawback as for the birth/death moves of section 3.2. Here we present some alternatives that are easier to implement.

In the set-up described in [10, 25], transitions from $\mathbf{s} \neq \emptyset$ to $\mathbf{s}' = (\mathbf{s} \setminus \{\eta\}) \cup \{\zeta\}$ for $\eta \in \mathbf{s}$ and $\zeta \in S = K \times [l_{\min}, l_{\max}] \times [0, \pi)$ are governed by the proposal kernel $c(\mathbf{s}, \eta, \zeta)$ and acceptance probabilities $\alpha(\mathbf{s}, (\mathbf{s} \setminus \{\eta\}) \cup \{\zeta\})$. Thus, for each choice of $\mathbf{s} \in \Omega$ and $\eta \in \mathbf{s}$, $c(\mathbf{s}, \eta, \cdot)$ is a probability density (with respect to the intensity measure of the reference Poisson process law μ) governing the change of $\eta \in \mathbf{s}$, and the proposal to replace η by ζ is accepted with probability $\alpha(\mathbf{s}, (\mathbf{s} \setminus \{\eta\}) \cup \{\zeta\})$. If a member η of configuration \mathbf{s} is selected for modification with probability $q(\mathbf{s}, \eta)$, the detailed balance equations require that $p(\mathbf{s}) q(\mathbf{s}, \eta) c(\mathbf{s}, \eta, \zeta) \alpha(\mathbf{s}, (\mathbf{s} \setminus \{\eta\}) \cup \{\zeta\}) = p((\mathbf{s} \setminus \{\eta\}) \cup \{\zeta\}) q((\mathbf{s} \setminus \{\eta\}) \cup \{\zeta\}, \zeta) c((\mathbf{s} \setminus \{\eta\}) \cup \{\zeta\}, \zeta, \eta) \alpha((\mathbf{s} \setminus \{\eta\}) \cup \{\zeta\}, \mathbf{s})$ whenever $p(\mathbf{s}), p((\mathbf{s} \setminus \{\eta\}) \cup \{\zeta\}) > 0$. We assume the selection probabilities are strictly positive, and impose the condition that $c(\mathbf{s}, \eta, \zeta) > 0$ if and only if $c((\mathbf{s} \setminus \{\eta\}) \cup \{\zeta\}, \zeta, \eta) > 0$. In words, if $\eta \in \mathbf{s}$ may be changed into ζ , the reverse update is also possible. Then,

$$\alpha(\mathbf{s}, (\mathbf{s} \setminus \{\eta\}) \cup \{\zeta\}) := \min \left\{ 1, \frac{p((\mathbf{s} \setminus \{\eta\}) \cup \{\zeta\}) q((\mathbf{s} \setminus \{\eta\}) \cup \{\zeta\}, \zeta) c((\mathbf{s} \setminus \{\eta\}) \cup \{\zeta\}, \zeta, \eta)}{p(\mathbf{s}) q(\mathbf{s}, \eta) c(\mathbf{s}, \eta, \zeta)} \right\} \quad (3.9)$$

is well-defined and solves the detailed balance equations.

Within the general context described above, there are many valid choices for the proposal kernel. To implement uniformly distributed joint ‘local’ changes, let $C(\eta) = C_k(\eta_k) \times C_m(\eta_l, \eta_\theta) \subseteq K \times ([l_{\min}, l_{\max}] \times [0, \pi))$ be a neighborhood of the segment $\eta = (\eta_k, \eta_l, \eta_\theta)$ such that $\nu(C_k(\eta_k))$ and $\text{length}(C_m(\eta_l, \eta_\theta))$ are both strictly positive, and set

$$c(\mathbf{s}, \eta, (k, l, \theta)) = \frac{1\{k \in C_k(\eta_k)\}}{\nu(C_k(\eta_k))} \frac{(l_{\max} \Leftrightarrow l_{\min}) \pi 1\{(l, \theta) \in C_m(\eta_l, \eta_\theta)\}}{\text{length}(C_m(\eta_l, \eta_\theta))}.$$

In order to ensure reversibility, we have to require that $\zeta \in C(\eta)$ whenever $\eta \in C(\zeta)$. Typically, $C(\eta)$ will be relatively small and centered at η . If $C(\eta) = S$, the local character is lost, and a new segment is proposed uniformly over the whole space. The latter has the potential

advantage of moving faster through the state space, the former of fine tuning likely configurations without destroying the overall appearance of the network. If C_m is of Cartesian product form, and the proposal density factorizes with respect to its position, length and orientation component, the modification may be implemented sequentially.

Change transitions are also useful for performing a death followed by a birth in one step, especially if the acceptance probability for the death is low. Thus, as in section 3, let $b(\cdot, \cdot)$ and $d(\cdot, \cdot)$ be strictly positive, and set

$$q(\mathbf{s}, \eta) = d(\mathbf{s}, \eta); \quad c(\mathbf{s}, \eta, \zeta) = b(\mathbf{s} \setminus \{\eta\}, \zeta) \quad (3.10)$$

for the proposal to move from $\mathbf{s} \in \Omega$ to $(\mathbf{s} \setminus \{\eta\}) \cup \{\zeta\}$ for some $\eta \in \mathbf{s}$, $\zeta \in S$.

A second type of update is to change a single segment component, say the orientation. Thus, for each $\eta = (\eta_k, \eta_l, \eta_\theta) \in \mathbf{s} \in \Omega$, we define a probability density $c_\theta(\mathbf{s}, \eta, \cdot)$ with respect to the uniform distribution on $[0, \pi)$. Given a neighborhood $C_\theta(\eta_\theta) \subseteq [0, \pi)$ of η_θ with positive length, one might set

$$c_\theta(\mathbf{s}, \eta, \theta) = \frac{\pi 1\{\theta \in C_\theta(\eta_\theta)\}}{\text{length}(C_\theta(\eta_\theta))}. \quad (3.11)$$

If $C_\theta(\eta_\theta) = [0, \pi)$, the new orientation is sampled uniformly over its full range; more commonly, a value in some small neighborhood of the current one is proposed. Again, we denote the probability that $\eta \in \mathbf{s}$ is selected for modification by $q(\mathbf{s}, \eta)$, and assume positivity. Then, the detailed balance equations read

$$\begin{aligned} p(\mathbf{s}) q(\mathbf{s}, \eta) c_\theta(\mathbf{s}, \eta, \theta) \alpha(\mathbf{s}, (\mathbf{s} \setminus \{\eta\}) \cup \{(\eta_k, \eta_l, \theta)\}) = \\ p((\mathbf{s} \setminus \{\eta\}) \cup \{(\eta_k, \eta_l, \theta)\}) q((\mathbf{s} \setminus \{\eta\}) \cup \{(\eta_k, \eta_l, \theta)\}, (\eta_k, \eta_l, \theta)) \times \\ c_\theta((\mathbf{s} \setminus \{\eta\}) \cup \{(\eta_k, \eta_l, \theta)\}, (\eta_k, \eta_l, \theta), \eta_\theta) \alpha((\mathbf{s} \setminus \{\eta\}) \cup \{(\eta_k, \eta_l, \theta)\}, \mathbf{s}) \end{aligned}$$

whenever $p(\mathbf{s})$, $p((\mathbf{s} \setminus \{\eta\}) \cup \{(\eta_k, \eta_l, \theta)\})$ are positive. We assume that $c_\theta(\mathbf{s}, \eta, \zeta_\theta) > 0$ if and only if $c_\theta((\mathbf{s} \setminus \{\eta\}) \cup \{\zeta\}, \zeta, \eta_\theta) > 0$ whenever η and ζ differ only in their orientation component. Then,

$$\begin{aligned} \alpha(\mathbf{s}, (\mathbf{s} \setminus \{\eta\}) \cup \{\zeta\}) := \\ \min \left\{ 1, \frac{p((\mathbf{s} \setminus \{\eta\}) \cup \{\zeta\}) q((\mathbf{s} \setminus \{\eta\}) \cup \{\zeta\}, \zeta) c_\theta((\mathbf{s} \setminus \{\eta\}) \cup \{\zeta\}, \zeta, \eta_\theta)}{p(\mathbf{s}) q(\mathbf{s}, \eta) c_\theta(\mathbf{s}, \eta, \zeta_\theta)} \right\} \quad (3.12) \end{aligned}$$

is well-defined and solves the detailed balance equations.

Similarly, one may define a proposal density $c_k(\mathbf{s}, \eta, \cdot)$ with respect to ν on K for modifying the position of a segment, or $c_l(\mathbf{s}, \eta, \cdot)$ with respect to the uniform distribution on $[l_{\min}, l_{\max}]$ for the length.

3.3 Convergence

In this section, we investigate the limit behavior of the Metropolis–Hastings algorithm with transitions as described in sections 3.1 and 3.2. As before, write π for the law of the Candy model and denote the product measure on S by σ . More formally, the transition kernel is

$$\begin{aligned} P(\emptyset, F) &= p_b \int_S b(\emptyset, \eta) \alpha(\emptyset, \{\eta\}) 1_F(\{\eta\}) d\sigma(\eta) \\ &+ 1_F(\emptyset) \left[1 \Leftrightarrow p_b \int_S b(\emptyset, \eta) \alpha(\emptyset, \{\eta\}) d\sigma(\eta) \right] \quad (3.13) \end{aligned}$$

for $\mathbf{s} = \emptyset$, $F \in \mathcal{F}$, and $P(\mathbf{s}, F)$ equals

$$\begin{aligned}
& p_b \int_S b(\mathbf{s}, \eta) \alpha(\mathbf{s}, \mathbf{s}' := \mathbf{s} \cup \{\eta\}) 1_F(\mathbf{s}') d\sigma(\eta) + p_d \sum_{s_i \in \mathbf{s}} d(\mathbf{s}, s_i) \alpha(\mathbf{s}, \mathbf{s}' := \mathbf{s} \setminus \{s_i\}) 1_F(\mathbf{s}') \\
& + p_c \sum_{s_i \in \mathbf{s}} q(\mathbf{s}, s_i) \int_S c(\mathbf{s}, s_i, \eta) \alpha(\mathbf{s}, \mathbf{s}' := (\mathbf{s} \setminus \{s_i\}) \cup \{\eta\}) 1_F(\mathbf{s}') d\sigma(\eta) + \\
& p_\theta \sum_{s_i \in \mathbf{s}} q(\mathbf{s}, s_i) \int_0^\pi c_\theta(\mathbf{s}, s_i, \theta) \alpha(\mathbf{s}, \mathbf{s}' := (\mathbf{s} \setminus \{s_i\}) \cup \{(s_{ik}, s_{il}, \theta)\}) 1_F(\mathbf{s}') \frac{d\theta}{\pi} + \\
& p_k \sum_{s_i \in \mathbf{s}} q(\mathbf{s}, s_i) \int_K c_k(\mathbf{s}, s_i, k) \alpha(\mathbf{s}, \mathbf{s}' := (\mathbf{s} \setminus \{s_i\}) \cup \{(k, s_{il}, s_{i\theta})\}) 1_F(\mathbf{s}') d\nu(k) + \\
& 1_F(\mathbf{s}) \left[1 \Leftrightarrow p_b \int_S b(\mathbf{s}, \eta) \alpha(\mathbf{s}, \mathbf{s} \cup \{\eta\}) d\sigma(\eta) \Leftrightarrow p_d \sum_{s_i \in \mathbf{s}} d(\mathbf{s}, s_i) \alpha(\mathbf{s}, \mathbf{s} \setminus \{s_i\}) + \right. \\
& \Leftrightarrow p_c \sum_{s_i \in \mathbf{s}} q(\mathbf{s}, s_i) \int_S c(\mathbf{s}, s_i, \eta) \alpha(\mathbf{s}, (\mathbf{s} \setminus \{s_i\}) \cup \{\eta\}) d\sigma(\eta) + \\
& \Leftrightarrow p_\theta \sum_{s_i \in \mathbf{s}} q(\mathbf{s}, s_i) \int_0^\pi c_\theta(\mathbf{s}, s_i, \theta) \alpha(\mathbf{s}, (\mathbf{s} \setminus \{s_i\}) \cup \{(s_{ik}, s_{il}, \theta)\}) \frac{d\theta}{\pi} + \\
& \left. \Leftrightarrow p_k \sum_{s_i \in \mathbf{s}} q(\mathbf{s}, s_i) \int_K c_k(\mathbf{s}, s_i, k) \alpha(\mathbf{s}, (\mathbf{s} \setminus \{s_i\}) \cup \{(k, s_{il}, s_{i\theta})\}) d\nu(k) \right] \quad (3.14)
\end{aligned}$$

otherwise. Here, p_c , p_θ and p_k are the probabilities of performing a change update, a modification of orientation and position respectively. The densities associated with the various transition proposals and the acceptance probabilities are as described in sections 3.1 and 3.2.

Let $L(\mathbf{s}, F)$ be the probability that the Markov chain started at $\mathbf{s} \in \Omega$ ever hits the set $F \in \mathcal{F}$. The chain is said to be *Harris recurrent* [9, 22] if $L(\mathbf{s}, F) = 1$ for all $\mathbf{s} \in \Omega$ and all $F \in \mathcal{F}$ with $\pi(F) > 0$. In words, all π -positive sets F are almost surely reached eventually from every initial state. Moreover, such sets will be visited infinitely often [22, 24]. The weaker condition of π -irreducibility requires only $L(\mathbf{s}, F) > 0$ for all $\mathbf{s} \in \Omega$ and all π -positive F , or equivalently $P^n(\mathbf{s}, F) > 0$ for some $n \in \mathbb{N}_0$.

An even stronger property than Harris recurrence is *geometric ergodicity* [22], that is geometric convergence in total variation:

$$\|P^n(\mathbf{s}, \cdot) \Leftrightarrow \pi\|_{TV} \leq c(\mathbf{s}) \gamma^n$$

for some constant $\gamma < 1$ and some π -integrable, non-negative function c . This property is important in establishing a central limit theorem for the sample path average of certain π -integrable functions [9, 22, 24]. Geometric ergodicity can be proved by means of the so-called geometric drift condition [22]. In order to state this condition, we need to recall the concept of a small set. A set C is *small* if $\pi(C) > 0$ and there exists a probability measure φ on \mathcal{F} , a constant $\epsilon > 0$, and an integer $n \in \mathbb{N}_0$ such that

$$P^n(\mathbf{s}, F) \geq \epsilon \varphi(F)$$

for all $\mathbf{s} \in C$ and all $F \in \mathcal{F}$. Now, the geometric drift condition entails the existence of a function $V : \Omega \rightarrow [1, \infty)$, constants $a < 1$ and $b < \infty$, and a small set $C \in \mathcal{F}$ such that

$$\int_{\Omega} V(\mathbf{s}') P(\mathbf{s}, d\mathbf{s}') \leq a V(\mathbf{s}) + b 1\{\mathbf{s} \in C\} \quad (3.15)$$

for all $\mathbf{s} \in \Omega$.

For further details on Markov chains on general state spaces, see e.g. the textbook by Meyn and Tweedie [22].

Theorem 3. *Let the functions b, d, c, c_θ, c_k and α be as described in sections 3.1–3.2, and in particular suppose that the birth proposal density and the death proposal probabilities are strictly positive. Assume that*

$$u_n = \sup_{\eta \in S, \mathbf{s} \in S_n} \frac{d(\mathbf{s}, \eta)}{b(\mathbf{s}, \eta)} \rightarrow 0$$

as $n \rightarrow \infty$, and that $p_b + p_d + p_c + p_k + p_\theta = 1$ with $p_b, p_d \in (0, 1)$ and $p_c, p_k, p_\theta \in [0, 1)$. Then the Metropolis–Hastings sampler for the Candy model (1.1) defined by (3.13)–(3.14) is geometrically ergodic.

The proof is an adaptation to the Candy model of the proof of [9, Proposition 3].

Proof: By lemma 3, the Candy model is locally stable. Let $\lambda > 0$ be an upper bound to the likelihood ratio, and set $V(\mathbf{s}) = A^{n(\mathbf{s})}$ for some $A > 1$.

The acceptance probability (3.5) for adding $\eta \notin \mathbf{s}$ to \mathbf{s} is

$$\min \left\{ 1, \frac{d(\mathbf{s}, \eta) p_d p(\mathbf{s} \cup \{\eta\})}{b(\mathbf{s}, \eta) p_b p(\mathbf{s})} \right\} \leq \frac{p_d \lambda}{p_b} \times u_{n(\mathbf{s})},$$

which, as u_n tends to 0, does not exceed a prefixed constant $\epsilon > 0$ if $n(\mathbf{s})$ is sufficiently large. Similarly, the acceptance probability for removing $\eta \notin \mathbf{s}$ from $\mathbf{s} \cup \eta$ equals

$$\min \left\{ 1, \frac{b(\mathbf{s}, \eta) p_b p(\mathbf{s})}{d(\mathbf{s}, \eta) p_d p(\mathbf{s} \cup \{\eta\})} \right\} \geq \min \left\{ 1, \inf \left[\frac{b(\mathbf{s}, \eta)}{d(\mathbf{s}, \eta)} \right] \times \frac{p_b}{p_d \lambda} \right\}$$

which reduces to 1 since the assumptions of the theorem imply

$$\inf \frac{b(\mathbf{s}, \eta)}{d(\mathbf{s}, \eta)} \rightarrow \infty$$

as $n(\mathbf{s})$ tends to infinity.

For the Metropolis–Hastings transition kernel P ,

$$\begin{aligned} \int_{\Omega} V(\mathbf{s}') P(\mathbf{s}, d\mathbf{s}') &= p_b A^{n(\mathbf{s})} \int_S b(\mathbf{s}, \eta) (A \Leftrightarrow 1) \alpha(\mathbf{s}, \mathbf{s} \cup \{\eta\}) d\sigma(\eta) \\ &+ p_d A^{n(\mathbf{s})} \sum_{\eta \in \mathbf{s}} d(\mathbf{s}, \eta) (A^{-1} \Leftrightarrow 1) \alpha(\mathbf{s}, \mathbf{s} \setminus \{\eta\}) + A^{n(\mathbf{s})}. \end{aligned} \quad (3.16)$$

For line segment configurations \mathbf{s} of sufficiently large cardinality, say $n(\mathbf{s}) > N_\epsilon$, $\alpha(\mathbf{s}, \mathbf{s} \setminus \{\eta\}) = 1$ and $\alpha(\mathbf{s}, \mathbf{s} \cup \{\eta\}) \leq \epsilon$, hence, recalling $A > 1$, (3.16) is less than or equal to

$$[p_b (A \Leftrightarrow 1) \epsilon + p_d (A^{-1} \Leftrightarrow 1) + 1] V(\mathbf{s}).$$

Since we have not yet specified ϵ , and the multiplier of $V(\mathbf{s})$ in the right hand side converges to $1 + p_d (A^{-1} \Leftrightarrow 1) = p_b + p_c + p_k + p_\theta + p_d/A < 1$ as ϵ tends to zero, we can pick ϵ such that $\int_{\Omega} V(\mathbf{s}') P(\mathbf{s}, d\mathbf{s}') \leq a V(\mathbf{s})$ for some $a < 1$.

Now, the set $C = \{\mathbf{s} \in \Omega : n(\mathbf{s}) \leq N_\epsilon\}$ is small. Indeed, the acceptance probability of a down step exceeds $\delta := \min\{p_b/(u_n p_d \lambda) : n \leq N_\epsilon\}$. Without loss of generality, δ is strictly less than 1. Moreover, $P(\emptyset, S_0) \geq p_d$. Hence,

$$P^{N_\epsilon}(\mathbf{s}, S_0) \geq P^{n(\mathbf{s})}(\mathbf{s}, S_0) P^{N_\epsilon - n(\mathbf{s})}(\emptyset, S_0) \geq (p_d \delta)^{N_\epsilon}$$

for any configuration \mathbf{s} consisting of at most N_ϵ segments. Hence, C is small with scalar multiplier $(p_d \delta)^{N_\epsilon}$ to the Dirac measure on \emptyset .

We have seen that (3.15) is satisfied for $\mathbf{s} \notin C$. For $\mathbf{s} \in C$, the geometric drift condition holds if we take $b = A^{N_\epsilon + 1}$. \square

Since self-transitions occur with positive probability, the Metropolis–Hastings chain is aperiodic, and the proof of theorem 3 implies the chain is Harris recurrent [9].

3.4 Discussion

In the preceding sections we discussed a range of updates that may be used as ingredients for a Metropolis–Hastings sampler. Although we tried to be rather general, yet other type of moves can be envisaged. For instance, it is possible to merge two close segments into one, or reversely split a large one in two [15, 32, 33, 34]. However, one would have to be careful in order to guarantee that the length of the new segment is in the interval $[l_{\min}, l_{\max}]$. It would also be possible to update several segments at the same time.

It is important to stress that a uniformly optimal sampler does not exist. For $\gamma_i = 1$ for $i = 1, \dots, 4$, the Candy model reduces to a Poisson line segment process, and simple uniform birth and death proposals will suffice. For stronger interaction, more weight should be given to updates that result in more likely patterns. In practice, in order to build a sampler that converges in a reasonable time, some experimentation is needed to find a balance between the various moves that accomplishes these objectives.

Finally, note that in order to assess whether the algorithm has converged, diagnostic tests based on the sufficient statistics of the model are widely used, see e.g. [36]. However, such tests only serve to falsify, that is indicate convergence is not reached yet. Theoretically, since the Candy model is locally stable (cf. lemma 3), coupling into and from the past [19, 29] can be used to obtain exact samples from (1.1), but due to the lack of monotonicity, it may be rather cumbersome in practice, especially in case of strong interaction between the segments.

4. MAXIMUM LIKELIHOOD ESTIMATION

The Candy model (1.1) is a five-parameter exponential family

$$p_\theta(\mathbf{s}) = \alpha(\theta) h(\mathbf{s}) \exp [t(\mathbf{s})^T \log \theta]$$

with normalizing constant $\alpha(\theta)$, $h(\mathbf{s}) = \prod_{i=1}^{n(\mathbf{s})} \exp \left[\frac{l_i - l_{\max}}{l_{\max}} \right]$, canonical sufficient statistic $t(S) = (n(S), n_f(S), n_s(S), n_r(S), n_o(S))^T$, and parameter vector $\theta = (\beta, \gamma_1, \gamma_2, \gamma_3, \gamma_4)^T$. Upon observing a pattern \mathbf{s} , consider the log likelihood ratio

$$l(\theta) = \log \frac{p_\theta(\mathbf{s})}{p_{\theta_0}(\mathbf{s})} = \log \frac{\alpha(\theta)}{\alpha(\theta_0)} + t(\mathbf{s})^T (\log \theta \Leftrightarrow \log \theta_0)$$

with respect to some reference value $\theta_0 \in (0, \infty) \times (0, 1)^4$. For notational convenience, from now on we shall write $\omega = \log \theta$ component wise. It is well known [9, 11] that $\alpha(\omega_0)/\alpha(\omega) = E_{\omega_0} \exp [t(S)^T (\omega \Leftrightarrow \omega_0)]$. Hence, the log likelihood ratio can be rewritten as follows

$$l(\omega) = t(\mathbf{s})^T (\omega \Leftrightarrow \omega_0) \Leftrightarrow \log E_{\omega_0} \exp [t(S)^T (\omega \Leftrightarrow \omega_0)] \quad (4.1)$$

from which it is easy to derive the score equations $\nabla l(\omega) = t(\mathbf{s}) \Leftrightarrow E_\omega t(S)$ and Fisher information matrix $\Leftrightarrow \nabla^2 l(\omega) = \text{Var}_\omega t(S)$. In summary, the maximum likelihood equations

$$E_\omega t(S) = t(\mathbf{s}) \quad (4.2)$$

state that under $\hat{\omega}$, the expected values of the sufficient statistics must be equal to the observed values. Now, since the covariance matrix of $t(S)$ is positive definite, (4.1) is concave in ω . Therefore, provided the score equations have a solution $\hat{\omega}$ in $\mathbb{R} \times \mathbb{R}_+^4$, a unique maximum likelihood estimator exists and equals $\hat{\omega}$. Otherwise, a maximum may be found on the boundary of the parameter space.

To solve (4.2), [8, 9, 11] suggested to approximate the expectation in (4.1) by its Monte Carlo counterpart $\sum_{i=1}^n \exp [t(S_i)^T (\omega \Leftrightarrow \omega_0)] / n$ based on a single sample S_1, \dots, S_n from p_{ω_0} . If we write $\hat{\omega}_n$ for the Monte Carlo approximation to the true maximum likelihood estimator $\hat{\omega}$, under mild regularity conditions [8, Theorem 7], this Monte Carlo maximum likelihood estimator is consistent and satisfies the following central limit theorem

$$\sqrt{n} (\hat{\omega}_n \Leftrightarrow \hat{\omega}) \rightarrow \mathcal{N}(0, I(\hat{\omega})^{-1} \Sigma I(\hat{\omega})^{-1})$$

where Σ is the asymptotic covariance matrix of the normalized Monte Carlo score $\sqrt{n} \nabla l_n(\hat{\omega})$ and $I(\hat{\omega}) = \text{Var}_{\hat{\omega}} t(S) = \Leftrightarrow \nabla^2 l(\hat{\omega})$ denotes the Fisher information matrix at the maximum likelihood estimator. Clearly, $I(\hat{\omega})$ can be estimated by

$$\Leftrightarrow \nabla^2 l_n(\hat{\omega}_n) = \frac{\frac{1}{n} \sum_{i=1}^n (t(\mathbf{s}) \Leftrightarrow t(S_i))^2 \exp [t(S_i)^T (\hat{\omega}_n \Leftrightarrow \omega_0)]}{\frac{1}{n} \sum_{i=1}^n \exp [t(S_i)^T (\hat{\omega}_n \Leftrightarrow \omega_0)]}$$

where as before S_1, \dots, S_n is a sample from p_{ω_0} ; an estimator for Σ is given by

$$\frac{\frac{1}{n} \sum_{i=1}^n (t(\mathbf{s}) \Leftrightarrow t(S_i))^2 \exp [2t(S_i)^T (\hat{\omega}_n \Leftrightarrow \omega_0)]}{\left\{ \frac{1}{n} \sum_{i=1}^n \exp [t(S_i)^T (\hat{\omega}_n \Leftrightarrow \omega_0)] \right\}^2}.$$

Importance sampling (4.1) relies on a reference value ω_0 that is not too far from the maximum likelihood estimator. One could use a grid of such values, with linear interpolation, or use a preliminary iteration. The Monte Carlo Newton–Raphson method [26] iteratively updates the parameters by

$$\omega_{k+1} = \omega_k \Leftrightarrow \nabla^2 l_n(\omega_k)^{-1} \nabla l_n(\omega_k)$$

$k = 1, 2, \dots$, where $l_n(\cdot)$ denotes the Monte Carlo approximation to the log likelihood (4.1) based on a sample of size n from p_{ω_k} . Since $\nabla l(\omega_k) = t(\mathbf{s}) \Leftrightarrow E_{\omega_k} t(S)$, another possibility is to set

$$\omega_{k+1} = \omega_k + \epsilon_k [t(\mathbf{s}) \Leftrightarrow t(S_k)]$$

for decreasing step sizes $\epsilon_k > 0$ and single realizations S_k from p_{ω_k} , a technique known as stochastic approximation [23, 39]. As k tends to infinity, under regularity conditions, ω_k approaches the maximum likelihood estimator, but no central limit theorem appears to be known for either method, although recent hybrid stochastic approximation techniques seem promising [5, 16]. Here we use the iterative gradient method, a variation on Newton–Raphson that guarantees convergence towards the local optimum in the vicinity of the initial point ω_1 [3, 28], i.e.

$$\begin{cases} l_n(\omega_k + \rho(\omega_k) \nabla l_n(\omega_k)) = \max_{\rho \in \mathbb{R}} l_n(\omega_k + \rho \nabla l_n(\omega_k)) \\ \omega_{k+1} = \omega_k + \rho(\omega_k) \nabla l_n(\omega_k) \end{cases} \quad (4.3)$$

where $\rho(\omega_k)$ is computed using a one-dimensional minimization of the log likelihood ratio. With occasional re-sampling to avoid numerical instability, the following algorithm [6, 36] was used.

1. Initialize ω_1 and $k = 1$;
2. Generate a sample of size n from p_{ω_k} and compute $\nabla l_n(\omega_k)$;
3. For every component $i = \{1, \dots, 5\}$ and gradient component Δ_i , compute the intervals $I_k^i = [\omega_k^i \Leftrightarrow \lambda \Delta_i, \omega_k^i + \lambda \Delta_i]$ with scalar precision parameter $\lambda > 0$, and maximize the log likelihood ratio in every such interval by golden section search to obtain a new value ω_{k+1} ;
4. If $\|\omega_{k+1} \Leftrightarrow \omega_k\| > T_1$, then $k = k + 1$ and go to the step 2. T_1 is a fixed threshold;
5. If $\|\nabla l_n(\omega_{k+1}) \Leftrightarrow \nabla l_n(\omega_k)\| > T_2$, then $k = k + 1$ and go to the step 3, else stop the algorithm. T_2 is a fixed threshold.

5. EXAMPLES

This section is devoted to a simulation study of the Candy model, a realization of which is shown in figure 3. The parameters are given in the figure, writing $\omega_t = \log \beta$, and n_t for the total number of points. We suppress the dependence of the sufficient statistics on the realization for brevity. Throughout, the point space $K = [0, 256] \times [0, 256]$, and marks take values in $[30, 40] \times [0, \pi)$. The connection radius is $r_c = 1/\sqrt{\pi}$. The threshold values δ_{\min} and τ_{\max} are 0.05π and 0.2π respectively.

In our first experiment, we ran the Metropolis-Hastings algorithm defined by the kernel (3.14) with $p_b = 0.6$, $p_d = 0.2$, $p_c = 0.1$, $p_\theta = 0.1$ and $p_k = 0.0$ from an empty initial configuration for 2×10^7 iterations, sub sampling the sufficient statistics every 10^3 steps. The birth proposal density $b(\mathbf{s}, \eta)$ was a mixture of (3.2) and (3.7) with respective weights

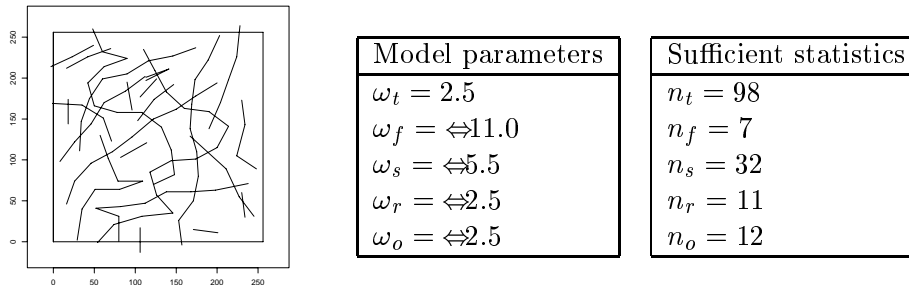


Figure 3: Realization (left) of the Candy model with parameter values as listed in the middle table. The observed values of the sufficient statistics are listed in the rightmost table.

$p_{1b} = 0.2$ and $p_{2b} = 0.8$; for the network extension, we used the uniform laws (3.8) and $p_M = p_{\tilde{M}} = 0.5$. For a configuration \mathbf{s} the set $A(\mathbf{s})$ is the union of all the extremities of the segments which are not connected and which are further than $\frac{1}{2}l_{\max} + r_c$ to the boundary of K .

The death proposal probabilities were as in (3.3). Regarding the change updates, in all cases $q(\mathbf{s}, s_i) = 1/n(\mathbf{s})$, while $c(\mathbf{s}, s_i, \eta) = b(\mathbf{s} \setminus \{s_i\}, \eta)$ and $c_\theta(\mathbf{s}, s_i, \theta)$ was as in (3.11) with $C_\theta(s_{i_\theta}) = [0, \pi)$.

Figure 4 gives an idea of how the topology of typical configurations depends upon the model parameters. It can be seen that the connectivity of the network can be controlled by the parameters ω_c and ω_f , the curvature by ω_o, ω_r , and the density by ω_t .

Our second experiment aimed to assess the performance of the Metropolis–Hastings algorithm by investigating the effect of the initial configuration and the various move types on the convergence speed. Figures 5 and 6 show realizations of the reference Candy model (parameters as in figure 3) obtained by the sampler described above, but initialized respectively with a realization of a binomial process consisting of 200 line segments and a random network rather than an empty configuration. To obtain the random network, we ran the Metropolis–Hastings sampler using change moves only, i.e. $p_b = p_d = p_k = 0.0$, $p_c = 0.5$, $p_\theta = 0.5$ with $c(\mathbf{s}, s_i, \eta)$ and $c_\theta(\mathbf{s}, s_i, \eta)$ as before and a realization of a binomial process of 200 points as initial state. As for figure 3, we carried out 2×10^7 iterations; the sufficient statistics were sub sampled every 10^3 steps. The estimated means $\bar{n}_t, \dots, \bar{n}_o$ of the sufficient statistics based on the three runs are close, and their evolution during the simulation does not seem to evoke doubts about convergence.

Next, we varied the mixture weights of the various moves. Figure 7 shows a realization and time series of the cumulative means for the weights $p_b = 0.45$, $p_d = 0.15$, $p_c = 0.3$, $p_\theta = 0.1$. In figure 8 the modified weights were $p_b = 0.7$, $p_d = 0.1$, $p_c = 0.1$, and $p_\theta = 0.1$. In both cases, $p_k = 0$, and $p_{1b} = 0.2$, $p_{2b} = 0.8$, $p_M = p_{\tilde{M}} = 0.5$.

The results indicate that neither the choice of initial state nor that of the mixture weights

is crucial in the investigated range. However, p_{2b} should not drop so far as to effectively exclude the tailored moves, as we show in figure 9, a simulation in which only uniform birth and death moves were used (i.e. $p_b = 0.75, p_d = 0.25$ and $p_{1b} = 1.0, p_{2b} = 0.0 = p_c = p_\theta = p_k$).

From the plots, it can be observed that after a large number of iterations a connected network emerges, but that the evolution of the sufficient statistics still indicates non-stationarity, in contrast to the previous examples.

To illustrate parameter estimation (section 4), suppose the data consist of the segment pattern shown in figure 3. We implemented the procedure explained in section 4, and initialized the iterative gradient algorithm (4.3) with arbitrary initial values listed in the first column of figure 10. For the fixed thresholds $\lambda = 10^{-3}$, $T_1 = 3.0$ and $T_2 = 10^{-6}$, we obtained the output shown in figure 10 (second column). Taking these values as reference parameter, we computed the Monte Carlo log likelihood ratio based on a Metropolis–Hastings run of 2×10^7 iterations, sub sampling the sufficient statistics every 10^3 steps. The weights of the various moves were the same as in the simulation of the reference model in figure 3. Cross sections of the Monte Carlo log likelihood ratio thus obtained are presented in figure 11. The maximum of $l_n(\omega)$ is located at $\hat{\omega}^n$, which vector is listed in the third column of figure 10. The asymptotic standard deviation of the unknown maximum likelihood estimator $\hat{\omega}$, and the Monte Carlo standard error (MCSE) are tabulated in figure 12.

6. CONCLUSION

In the first part of this paper, we recalled the definition of the Candy model, and studied its analytical properties, concentrating on the Ruelle condition, local stability and Markov properties. The second part was devoted to statistical inference by Markov chain Monte Carlo. We suggested a variety of tailor-made updates, and proved convergence of the resulting transition kernel. Finally, we applied the sampler in a parameter estimation scheme, and performed a simulation study which shows the importance of a reasonable mix of updates that balance quick moves through the state space with tailor build ones for fine tuning and enhancement. The relative weights of the moves may be adapted to the model parameters. Simple statistics, such as the number of free segments, converge faster than more complex ones like the average fraction of doubly connected segments.

Since the Candy model was conceived in the context of road extraction from satellite images, we expect the results presented in this paper to be a starting point in unsupervised network extraction. This can be done by adding to the Candy model a term [36, 37] which adapts the location of the road network to the data. As road density depends on geographical location, we expect to be able to improve the detection by defining a Candy model with respect to a non-homogeneous Poisson point process [38]. Another important point is to study the feasibility of exact simulation algorithms for the Candy model.

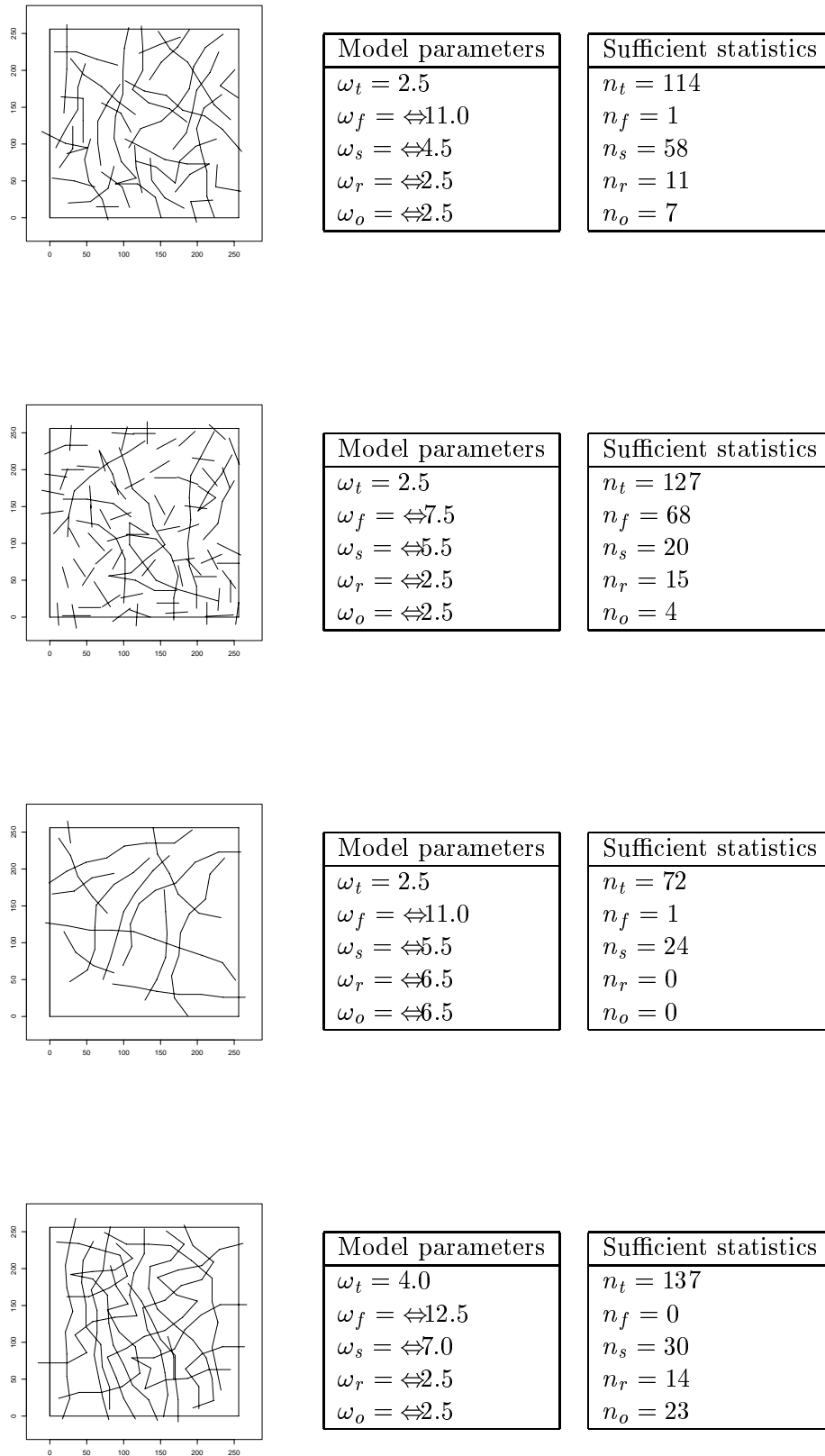


Figure 4: Realizations (left plot) of the Candy model for a range of parameters values (middle table) with observed values of the sufficient statistics (right table).

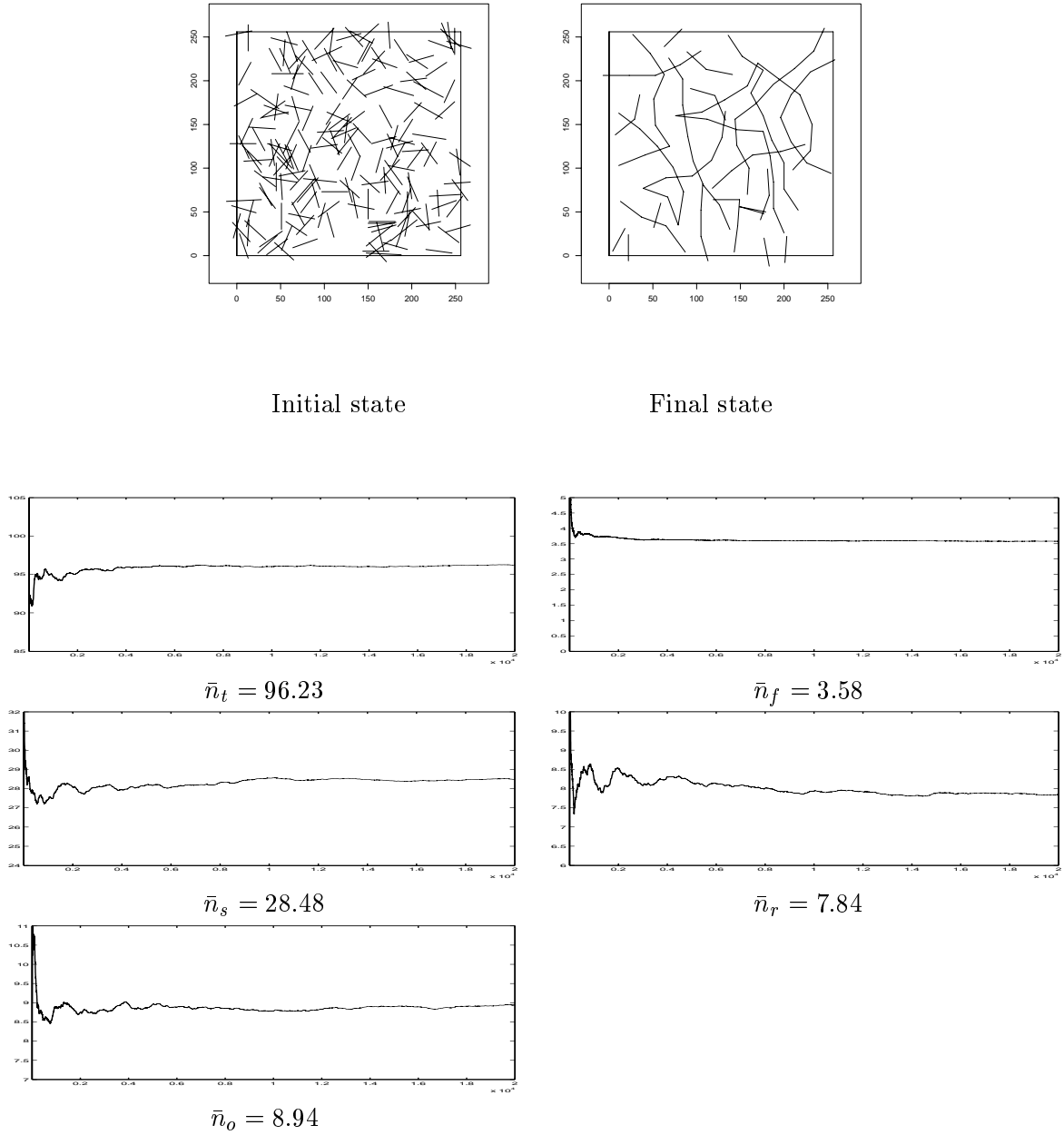


Figure 5: Time series of the cumulative means of the sufficient statistics during a run of the Metropolis–Hastings sampler described in the text. The initial state (a realization of a binomial process of 200 segments) is shown in the top left plot, the final configuration in the top right figure.

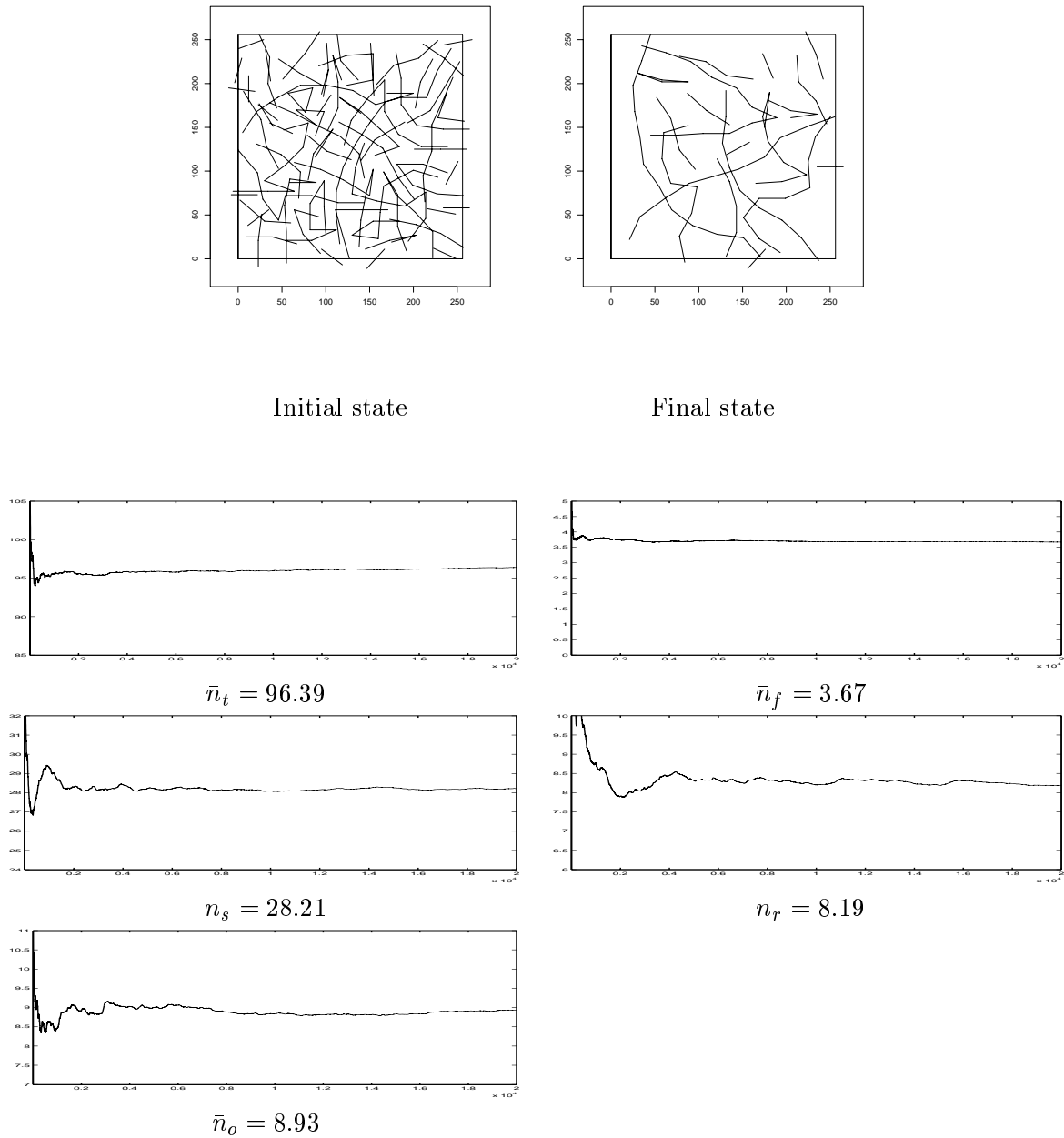


Figure 6: Time series of the cumulative means of the sufficient statistics during a run of the Metropolis–Hastings sampler described in the text. The initial state is shown in the top left plot, the final configuration in the top right figure.

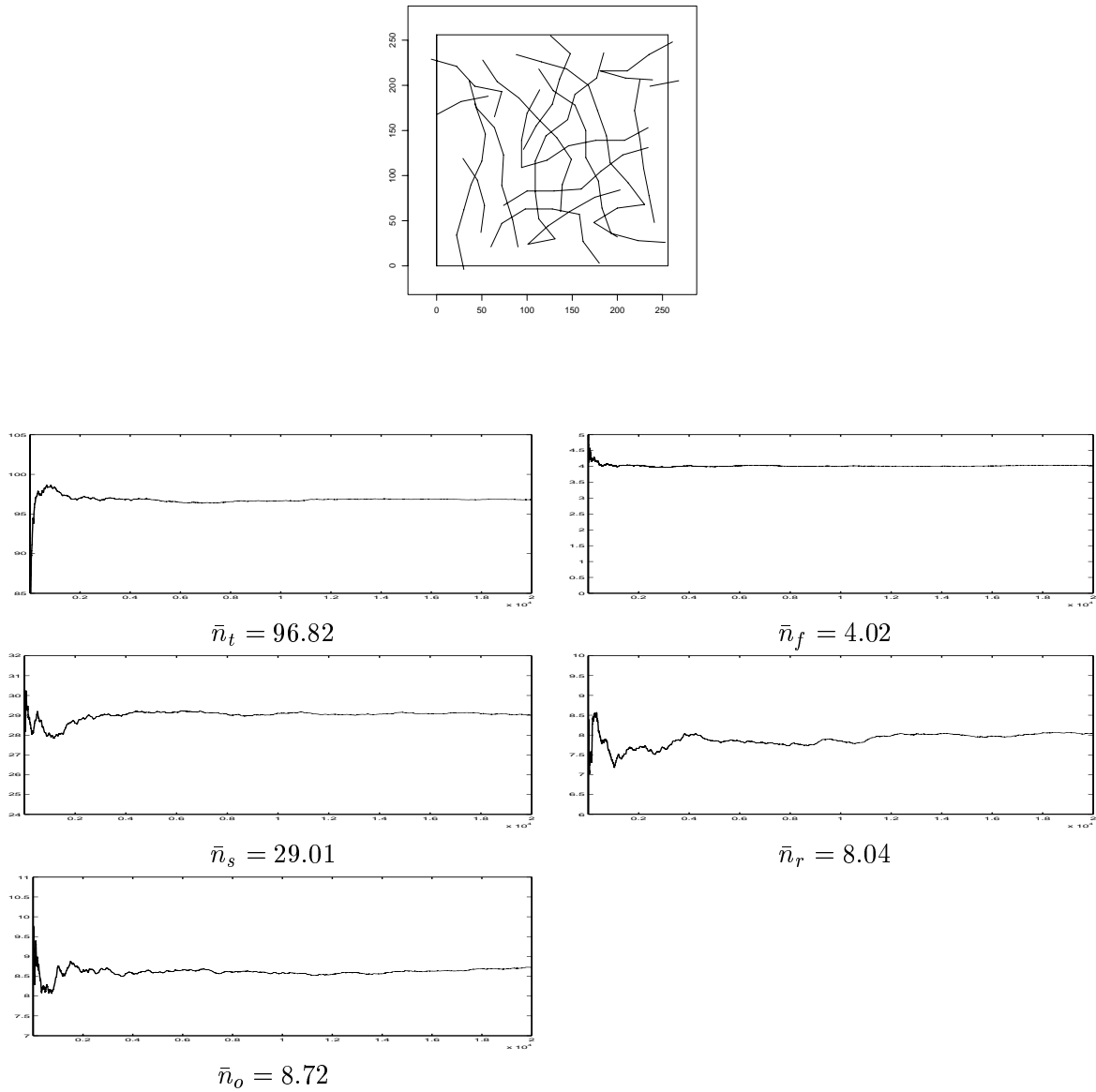


Figure 7: Time series of the cumulative means of the sufficient statistics during a run of the Metropolis-Hastings sampler with mixture weights $p_b = 0.45$, $p_d = 0.15$, $p_c = 0.3$, $p_\theta = 0.1$. The initial state is the empty configuration, the final configuration is plotted in the top figure.

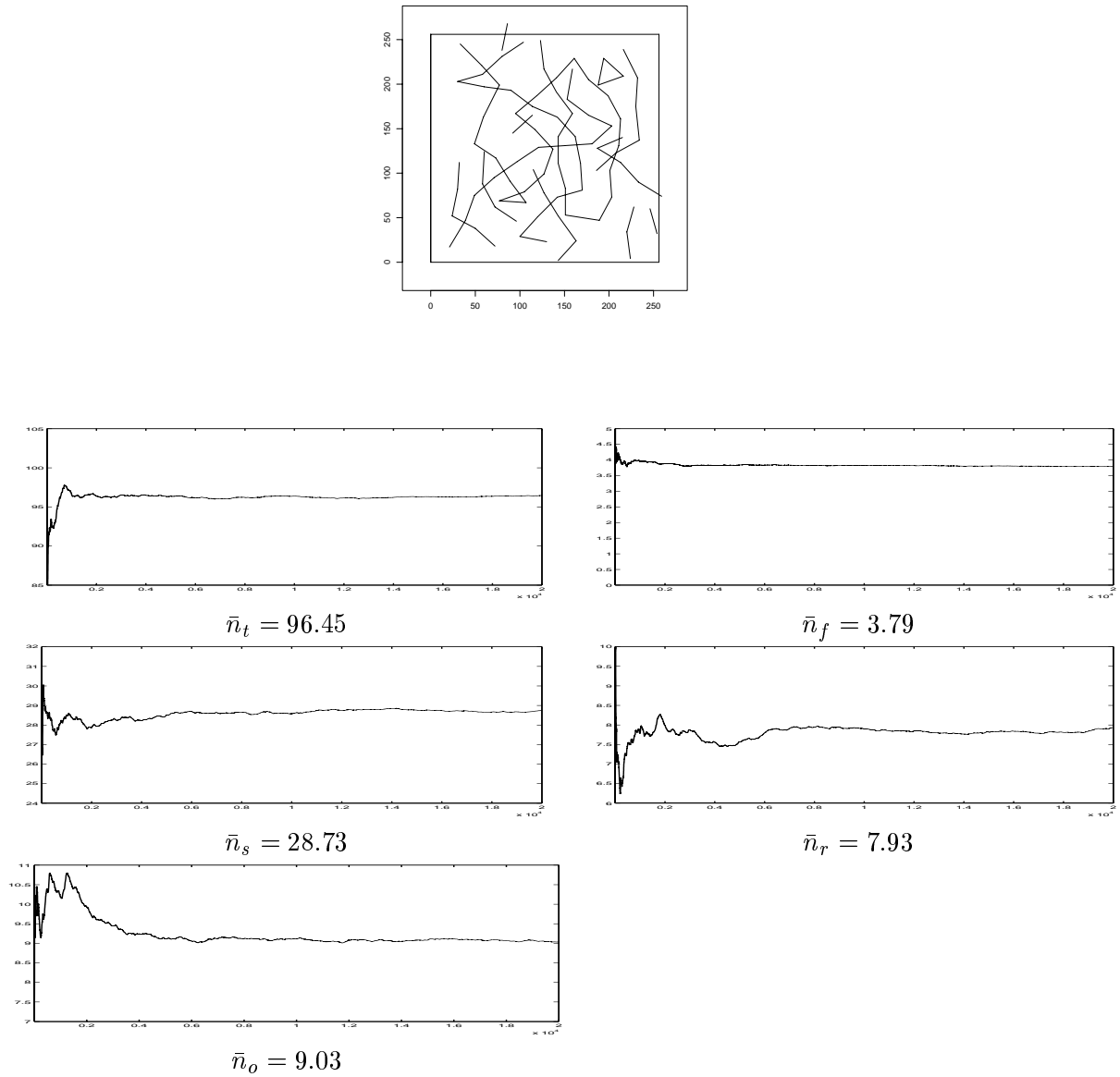


Figure 8: Time series of the cumulative means of the sufficient statistics during a run of the Metropolis–Hastings sampler with mixture weights $p_b = 0.7$, $p_d = 0.1$, $p_c = 0.1$, $p_\theta = 0.1$. The initial state is the empty configuration, the final configuration is plotted in the top figure.

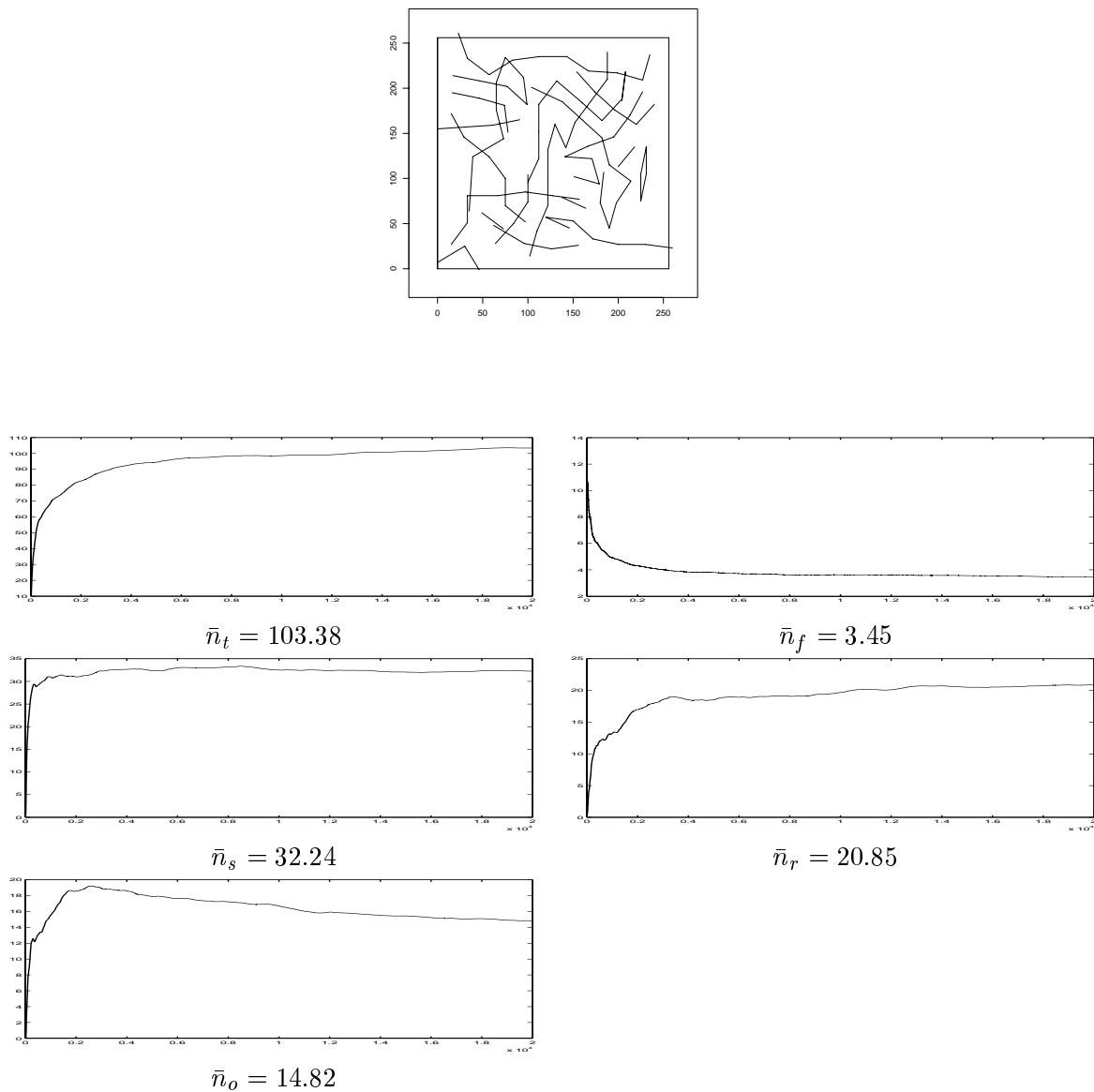
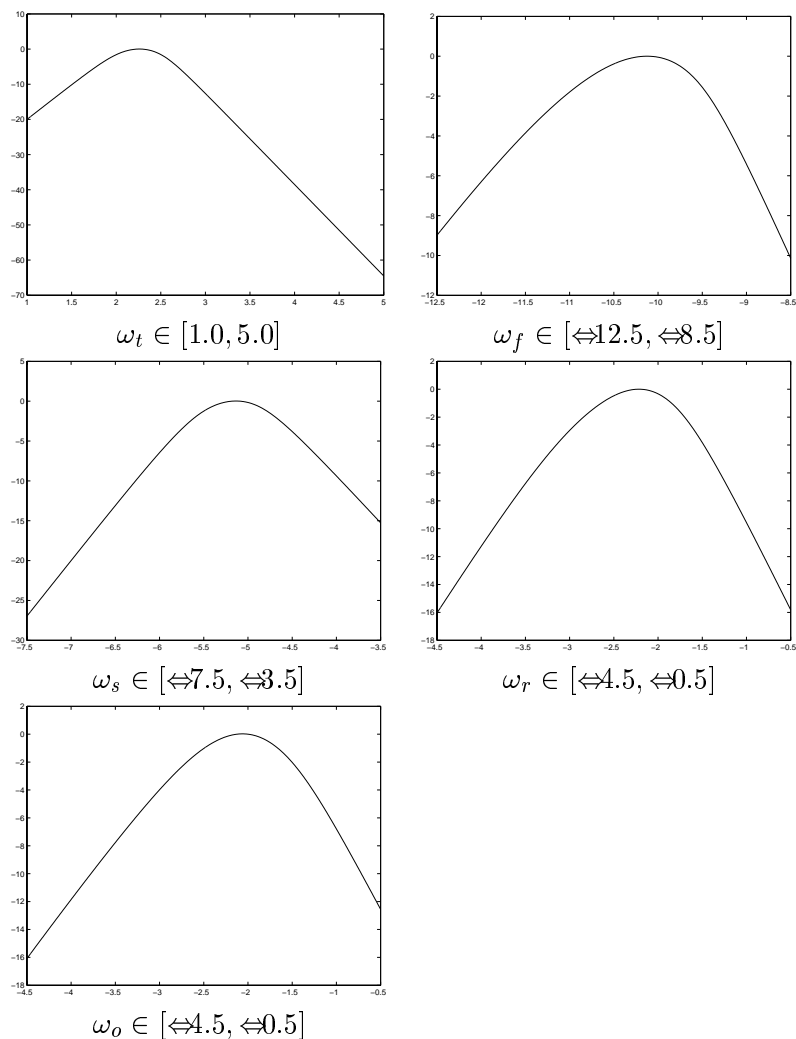


Figure 9: Time series of the cumulative means of the sufficient statistics during a run of the Metropolis–Hastings sampler with mixture weights $p_b = 0.75$, $p_d = 0.25$ and $p_{1b} = 1.0$, $p_{2b} = p_c = p_\theta = 0.0$. The initial state is the empty configuration, the final configuration is plotted in the top figure.

Initial value	Iterative method	Monte Carlo MLE
$\omega_t^i = 1.5$	$\hat{\omega}_t^0 = 2.28$	$\hat{\omega}_t^n = 2.24$
$\omega_f^i = \Leftrightarrow 11.00$	$\hat{\omega}_f^0 = \Leftrightarrow 10.11$	$\hat{\omega}_f^n = \Leftrightarrow 10.08$
$\omega_s^i = \Leftrightarrow 5.5$	$\hat{\omega}_s^0 = \Leftrightarrow 5.18$	$\hat{\omega}_s^n = \Leftrightarrow 5.09$
$\omega_r^i = \Leftrightarrow 3.5$	$\hat{\omega}_r^0 = \Leftrightarrow 2.22$	$\hat{\omega}_r^n = \Leftrightarrow 2.23$
$\omega_o^i = \Leftrightarrow 3.5$	$\hat{\omega}_o^0 = \Leftrightarrow 2.00$	$\hat{\omega}_o^n = \Leftrightarrow 2.06$

Figure 10: Estimating the parameters for the data of figure 3.

Figure 11: Monte Carlo approximation of the log likelihood function for the data of figure 3. The X axis represents the variation of a single component. The Y axis represents the values of the Monte Carlo log likelihood with all other components of $\hat{\omega}^0$ fixed.

Asymptotic standard deviation	Monte Carlo standard deviation
0.17	0.004
0.39	0.002
0.25	0.003
0.33	0.002
0.29	0.004

Figure 12: Estimation errors.

References

1. A.J. Baddeley and J. Møller. Nearest-neighbour Markov point process and random sets. *International Statistical Review*, 57:89-121, 1989.
2. A.A. Barker. Monte Carlo calculation of the radial distribution functions for a proton-electron plasma. *Australian Journal of Physics*, 18:119-133, 1965.
3. P.G. Ciarlet. *Introduction à l'analyse numérique matricielle et à l'optimisation*. Masson, Paris, 1994.
4. D.J. Daley and D. Vere-Jones. *An introduction to the theory of point processes*. Springer Verlag, New York, 1988.
5. B. Delyon, M. Lavielle and E. Moulines. Convergence of a stochastic approximation version of the EM algorithm. *The Annals of Statistics*, 27:94-128, 1999.
6. X. Descombes, R.D. Morris, J. Zerubia and M. Berthod. Estimation of Markov random field prior parameters using Markov chain Monte Carlo maximum likelihood. *IEEE Transactions on Image Processing*, 8:954-963, 1999.
7. D.J. Gates and M. Westcott. Clustering estimates for spatial point distributions with unstable potentials. *Annals of the Institute of Statistical Mathematics*, 38:123-135, 1986.
8. C.J. Geyer. On the convergence of Monte Carlo maximum likelihood calculations. *Journal of the Royal Statistical Society, Series B*, 56:261-274, 1994.
9. C.J. Geyer. Likelihood inference for spatial point processes. In O. Barndorff-Nielsen, W.S. Kendall, and M.N.M. van Lieshout, editors, *Stochastic geometry, likelihood, and computation*, CRC Press/Chapman and Hall, Boca Raton, 1999.
10. C.J. Geyer and J. Møller. Simulation procedures and likelihood inference for spatial point processes. *Scandinavian Journal of Statistics*, 21:359-373, 1994.
11. C.J. Geyer and E.A. Thompson. Constrained Monte Carlo maximum likelihood for dependent data. *Journal of the Royal Statistical Society, Series B*, 54:657-699, 1992.
12. W.R. Gilks, S. Richardson, and D.J. Spiegelhalter. *Markov chain Monte Carlo in practice*.

- Chapman and Hall, London, 1996.
13. P. Grabarnik and A. Särkkä. Interacting neighbour point processes. To appear in *Journal of Statistical Computation and Simulation*.
 14. P.J. Green. Reversible jump MCMC computation and Bayesian model determination. *Biometrika*, 82:711–732, 1995.
 15. U. Grenander and M.I. Miller. Representations of knowledge in complex systems. *Journal of the Royal Statistical Society, Series B*, 56:549–603, 1994.
 16. M.G. Gu and H-T. Zhu. Maximum likelihood estimation for spatial models by Markov chain Monte Carlo stochastic approximation. *Journal of the Royal Statistical Society, Series B*, 63:339–355, 2001.
 17. W. Hastings. Monte Carlo sampling methods using Markov chains and their application. *Biometrika*, 57:97–109, 1970.
 18. M.M. Hayat and J.A. Gubner. A two-step Markov point process. Technical Report ECE-96-2, Department of Electrical Computer Engineering, University of Wisconsin-Madison, 1996.
 19. W.S. Kendall and J. Møller. Perfect Metropolis–Hastings simulation of locally stable spatial point processes. *Advances in Applied Probability (SGSA)*, 32:844–865, 2000.
 20. M.N.M. van Lieshout. *Markov point processes and their applications*. Imperial College Press/World Scientific Publishing, London/Singapore, 2000.
 21. N. Metropolis, A.W. Rosenbluth, M.N. Rosenbluth, A.H. Teller and E. Teller. Equation of state calculations by fast computing machines. *Journal of Chemical Physics*, 21:1087–1092, 1953.
 22. S.P. Meyn and R.L. Tweedie. *Markov chains and stochastic stability*. Springer-Verlag, London, 1993.
 23. R.A. Moyeed and A.J. Baddeley. Stochastic approximation of the MLE for a spatial point pattern. *Scandinavian Journal of Statistics*, 18:39-50, 1991.
 24. J. Møller. Markov chain Monte Carlo and spatial point processes. In O. Barndorff-Nielsen, W.S. Kendall, and M.N.M. van Lieshout, editors, *Stochastic geometry, likelihood, and computation*, CRC Press/Chapman and Hall, Boca Raton, 1999.
 25. Y. Ogata and M. Tanemura. Estimation for interaction potentials of spatial point patterns through the maximum likelihood procedure. *Annals of the Institute of Statistical Mathematics*, 33:315–338, 1981.
 26. A. Penttinen. *Modelling interaction in spatial point patterns: parameter estimation by the maximum likelihood method*. Jyväskylä Studies in Computer Science, Economics and Statistics (Vol. 7), University of Jyväskylä, 1984.
 27. P. Peskun. Optimum Monte Carlo sampling using Markov chains. *Biometrika*, 60:607–612, 1973.
 28. W.H. Press, B.P. Flannery, S.A. Teukolsky. *Numerical recipes in C : the art of scientific computing*. Cambridge University Press, 1988.
 29. J.G. Propp and D.B. Wilson. Exact sampling with coupled Markov chains and applica-

- tions to statistical mechanics. *Random Structures and Algorithms*, 9:223–252, 1996.
30. R.-D. Reiss. *A course on point processes*. Springer, New York, 1993.
 31. B.D. Ripley and F.P. Kelly. Markov point processes. *Journal of the London Mathematical Society*, 15:188–192, 1977.
 32. H. Rue and M.A. Hurn. Bayesian object identification. *Biometrika*, 3:649–660, 1999.
 33. H. Rue and O.K. Husby. Identification of partly destroyed objects using dynamic polygons. *Statistics and Computing*, 8:221–228, 1998.
 34. H. Rue and A.R. Syversveen. Bayesian object recognition with Baddeley’s Delta loss. *Advances in Applied Probability (SGSA)*, 30:64–84, 1998.
 35. D. Ruelle. *Statistical Mechanics*. Wiley, New York, 1969.
 36. R. Stoica. *Processus ponctuels pour l’extraction des réseaux linéiques dans les images satellitaires et aériennes*. PhD Thesis, University of Nice–Sophia Antipolis, 2001.
 37. R. Stoica, X. Descombes and J. Zerubia. A Gibbs point process for road extraction in remotely sensed images. Research Report 3923, INRIA Sophia Antipolis, 2000.
 38. D. Stoyan, H. Stoyan. Non-homogeneous Gibbs process models for forestry - a case study. *Biometrical Journal*, 40:521–531, 1998.
 39. L. Younes. Estimation and annealing for Gibbsian fields. *Annales de l’Institut Henri Poincaré, Probabilités et Statistiques*, 24:269–294, 1988.